Statistical Time Series Methods for Vibration Based Structural Health Monitoring

Spilios D. Fassois and Fotis P. Kopsaftopoulos
Stochastic Mechanical Systems & Automation (SMSA) Laboratory
Department of Mechanical & Aeronautical Engineering
University of Patras, 26504 Patras, Greece
E-mail: {fassois,fkopsaf}@mech.upatras.gr
Internet: www.smsa.upatras.gr

Abstract Statistical time series methods for vibration based structural health monitoring utilize random excitation and/or vibration response signals, statistical model building, and statistical decision making for inferring the health state of a structure. This includes damage detection, identification (including localization) and quantification. The principles and operation of methods that utilize the time or frequency domains are explained, and they are classified into various categories under the broad non-parametric and parametric classes. Representative methods from each category are outlined and their use is illustrated via their application to a laboratory truss structure.

1 Introduction

Structural Health Monitoring (SHM) involves the *continual* or *continuous* over time monitoring of a structure based on proper sensors which provide dynamic structural responses and other related data (such as environmental conditions), signal/data processing and analysis, as well as proper decision making for inferring the current health state of the structure. Once set up, an SHM procedure is ideally intended to be *global* (in the sense of covering the whole structure or a large part of it), *automated*, without necessitating human interaction, cost-effective, and capable of effectively treating the level I, II and III subproblems (Rytter, 1993), that is *damage detection* (simply detecting damage presence), *damage identification* (identifying the damage type/nature and location) and *damage quantification* (estimating the damage extent) – see section 2.2 for details.

Historically, SHM may be thought of as an evolution of classical Non-Destructive Testing (NDT) procedures (commonly based on ultrasound,

W. Ostachowicz, J. Güemes (Eds.), *New Trends in Structural Health Monitoring*,
CISM International Centre for Mechanical Sciences, DOI 10.1007/978-3-7091-1390-5_4,
© CISM, Udine 2013

acoustic, radiography, eddy current, and thermal field principles – Doherty 1987; Doebling et al. 1996, 1998; Farrar et al. 2001; Balageas et al. 2006). NDT is however different, in that it is exercised on demand – usually on a periodic basis – without permanent sensors mounted on the structure and not necessarily in an automated fashion. NDT typically works locally, requiring access to the vicinity of the suspected damage location, while the procedure is often time consuming and costly. On the other hand, the SHM philosophy and principles are much closer to the general theory of fault diagnosis (see Basseville and Nikiforov 1993; Rytter 1993; Doebling et al. 1996, 1998; Natke and Cempel 1997; Salawu 1997; Farrar et al. 2001).

Vibration based SHM is quite popular, as vibration is naturally available for many structures (aircraft, railway vehicles, bridges, and so on), while the technology for the precise measurement and processing of vibration signals has been available for a long time. For overviews of general vibration based methods see Doebling et al. (1996, 1998); Salawu (1997); Zou et al. (2000); Farrar et al. (2001); Sohn et al. (2003b); DeRoeck (2003); Carden and Fanning (2004); Montalvão et al. (2006). Also see Staszewski et al. (2004); Inman et al. (2005); Balageas et al. (2006); Fritzen (2006); Adams (2007).

Statistical time series SHM methods form an important and rapidly evolving class within the broader context of vibration based SHM. Their three *main elements* are: (i) random excitation and/or vibration response signals (referred to as *time series*), (ii) statistical model building, and (iii) statistical decision making for inferring the health state of a structure. As with all vibration based methods, the *fundamental principle* upon which they are founded is that small changes (damage) in a structure causes corresponding changes in the structural dynamics. These changes are reflected – though often in a very subtle form – in the measured vibration responses. Hence, the main idea is on the use of measured vibration signals in order to detect, identify, and quantify changes in the *underlying structural dynamics* which are attributed to damage. It could be argued that the effects of damage might be evident simply on the vibration response level, without the need for elaborate analysis. This was indeed used in the early days, and it might still be adequate in certain applications. The drawback of such a simple approach however is that the increased vibration level may be due to alternative reasons, such as increased excitation. Furthermore, modern SHM methods which are based on the dynamics aim at detecting damage at an *early stage*, well before increases in the vibration level are noticed. Statistical time series SHM methods are discussed in references such as Natke and Cempel (1997); Basseville et al. (2000); Sohn and Farrar (2000); Fugate et al. (2001); Yan et al. (2004); Carden and Brownjohn (2008) – see Fassois and Sakellariou (2007, 2009) for recent overviews.

From an *operational viewpoint*, statistical time series SHM methods involve two distinct phases: In an initial *baseline (training) phase*, the methods employ random excitation and/or vibration response (displacement, velocity or acceleration) signals obtained from the structure under its healthy state, as well as from a number of potential damage states, for identifying suitable non-parametric or parametric statistical time series models that describe the structural dynamics in each considered state. A statistical quantity, referred to as *characteristic quantity* and characterizing each structural state, is then extracted.

In the continually or continuously implemented *inspection phase*, the procedure is repeated under the current conditions using freshly measured signals. The current characteristic quantity is obtained, and damage detection, identification (including localization) and quantification (magnitude estimation) are accomplished via statistical decision making procedures consisting of "comparing", in a statistical sense, the current characteristic quantity with that of each potential structural state determined in the baseline phase.

Statistical time series SHM methods thus involve inverse type procedures, as the models employed are *data based* rather than physics based. In addition to the features of the general vibration based methods, statistical time series methods offer further unique *advantages* such as (Fassois and Sakellariou, 2007, 2009; Basseville et al., 2004; Sakellariou and Fassois, 2008; Kopsaftopoulos and Fassois, 2010):

(i) No need for physics based or analytical, such as Finite Element (FE), models.

(ii) No need for complete structural models. In fact models describing only part of the dynamics and based on a very limited number (even a single pair) of excitation and/or vibration response signals are sometimes adequate.

(iii) Inherent accounting for uncertainties (measurement, environmental, operational and so on) through statistical tools.

(iv) Statistical decision making with specified performance characteristics.

(v) Effective operation even in the "low" frequency range.

(iv) Effective use of naturally obtained random vibration signals. This is very important as it implies that there is no need for interrupting the normal operation of the structure.

Of course, like with any other family, statistical time series SHM methods have their limitations. Since only partial structural models are employed, they may identify (locate) damage only to the extent allowed by the type of model used. In addition, adequate "training" in the baseline phase is needed in order to tackle the damage identification and magnitude estimation subproblems, and sufficient user expertise is required.

The goal of this chapter is to provide an overview of the principles and main classes of statistical time series SHM methods. Simple *non-parametric*, as well as more advanced *parametric* methods are reviewed, while both the *response-only* and *excitation-response* measurement cases are considered. The methods are mainly presented for continual (periodic) inspection, although extensions to continuous (on-line) monitoring are possible (for instance through the use of a time window sliding over the measured signals).

For purposes of simplicity, the presentation is limited to the *single (scalar)* vibration signal case – extensions to the *multiple (vector)* signal case are available, and pertinent references are provided in the bibliographical remarks. Likewise, the presentation focuses on *time-invariant (stationary)* and *linear* structural dynamics in a *Gaussian* context, although – with proper modifications – the concepts may extend to the time-varying and non-linear cases. One important aspect, which due to space limitations is not covered in the chapter, is *environmental effects* or in broader terms the *effects of varying operating conditions.* These can be very important and – if not properly accounted for – they may have an adverse effect on SHM operation (Doebling et al., 1996; Sohn, 2007; Deraemaeker et al., 2008; Figueiredo et al., 2011).

The rest of this chapter is organized as follows: The general framework of the methods is presented in section 2. Non-parametric and parametric time series models for representing the structural dynamics are presented in section 3. Selected non-parametric and parametric time series SHM methods are presented in sections 4 and 5, respectively. The application of selected methods to damage diagnosis for a laboratory truss structure is presented in section 6. Concluding remarks are finally summarized in section 7.

2 The General Workframe

2.1 The Structural States and the Data Sets

Let S_o designate the structure under consideration in its *nominal* (healthy) state and S_u the structure in an unknown, to be determined, state. Furthermore, let $S_A, S_B, \ldots$ designate the structure under damage of type $A, B, \ldots$, respectively. Each damage type includes a continuum of damages of common nature or location but of any admissible damage magnitude.

Statistical time series SHM methods are typically based on discretized excitation $x[t]$ and/or response $y[t]$ (for $t = 1, 2, \ldots, N$) random vibration data records. The discrete time t corresponds to the actual time $(t-1) \cdot T_s$, with T_s designating sampling period. Let the complete excitation and

Table 1. Workframe setup: structural state, vibration signals used, and the characteristic quantity.

Baseline Phase			
Structural state	S_o (healthy structure)	S_A (damage type A)†	$\ldots$
Vibration signals	$z_o[t] = (x_o[t], y_o[t])$	$z_A[t] = (x_A[t], y_A[t])$	$\ldots$
	$Z_o = (X_o, Y_o)$	$Z_A = (X_A, Y_A)$	$\ldots$
Characteristic quantity	Q_o	Q_A	$\ldots$
Inspection Phase			
Structural state	S_u (current structure in unknown state)		
Vibration signals	$z_u[t] = (x_u[t], y_u[t])$		
	$Z_u = (X_u, Y_u)$		
Characteristic quantity	Q_u		

†Various damage magnitudes may be considered within each damage type.

response signals be designated as X and Y, respectively, or, collectively as $Z = (X, Y)$. The subscript $(o, A, B, \ldots, u)$ is used for designating the state of the structure that provided the signals.

All signals measured under the various structural states need to be suitably preprocessed (Doebling et al., 1996; Ljung, 1999; Fassois, 2001; Sohn, 2007). This may include low or bandpass filtering within the frequency range of interest, signal subsampling (in case the original sampling frequency is too high) and normalization, which includes sample mean subtraction and division by its sample standard deviation. Normalization is used in the linear case only, for improving numerical accuracy, but also counteracting different operating or environmental conditions or excitation levels.

2.2 The Baseline and Inspection Phases

As indicated, the methods consist of an initial *baseline phase*, while normal operation takes place under the continually or continuously implemented *inspection phase* (see Table 1). In the *baseline (training) phase* the data records $Z_o, Z_A, Z_B, \ldots$ are obtained and analyzed, while the data record Z_u, corresponding to an unknown (to be determined) structural state, is obtained and analyzed in the *inspection* phase. Based on each data record a non-parametric or parametric time series model representing part of the structural dynamics is identified and validated. From each estimated model, the corresponding estimate[1] of a *characteristic quantity* Q is extracted ($\widehat{Q}_o, \widehat{Q}_A, \widehat{Q}_B, \ldots$ in the baseline phase, and $\widehat{Q}_u$ in the inspection phase).

[1]Estimators/estimates are designated by a hat.

Table 2. The damage detection, identification, and estimation subproblems.

	Damage detection	
H_o :	$Q_u \sim Q_o$	Null hypothesis (healthy structure)
H_1 :	$Q_u \nsim Q_o$	Alternative hypothesis (damaged structure)
	Damage identification	
H_A :	$Q_u \sim Q_A$	Hypothesis A (damage type A)
H_B :	$Q_u \sim Q_B$	Hypothesis B (damage type B)
	$\vdots$	$\vdots$
	Damage estimation	
Estimate the damage magnitude given the damage type.		

$\sim$ indicates a proper relationship, such as equality, inequality and so on.

Damage detection, identification and quantification. *Damage detection* is then based on proper comparison of the true (but not precisely known) current characteristic quantity Q_u to the true (but also not precisely known) characteristic quantity Q_o of the healthy structure (Table 2). This is accomplished via a binary composite statistical hypothesis test that employs the corresponding estimates $\widehat{Q}_u$ and $\widehat{Q}_o$.

Damage identification is similarly based on proper comparison of the current characteristic quantity Q_u to each of $Q_A, Q_B, \ldots$ (Table 2) via statistical hypothesis testing that also employs the corresponding estimates. *Damage estimation (quantification)* generally is a more complicated task that requires proper formulation and the use of interval estimation techniques (Table 2). The workframe of a general statistical time series SHM method is presented in Figure 1.

The design of a binary statistical hypothesis test is generally based on two error probabilities:

(i) The *type I error* or *false alarm* probability, designated as α, which is the probability of rejecting the null hypothesis H_o when it is true.

(ii) The *type II error* or *missed damage* probability, designated as β, which is the probability of accepting the null hypothesis H_o when it is not true.

The majority of the designs presented herein are based on the type I error probability α. In selecting α it should be noted that as it decreases (resp. increases), β increases (resp. decreases). The reader is referred to Lehmann and Romano (2008), Basseville and Nikiforov (1993, section 4.2), and Montgomery (1991, section 3.3) for details on statistical hypothesis testing.

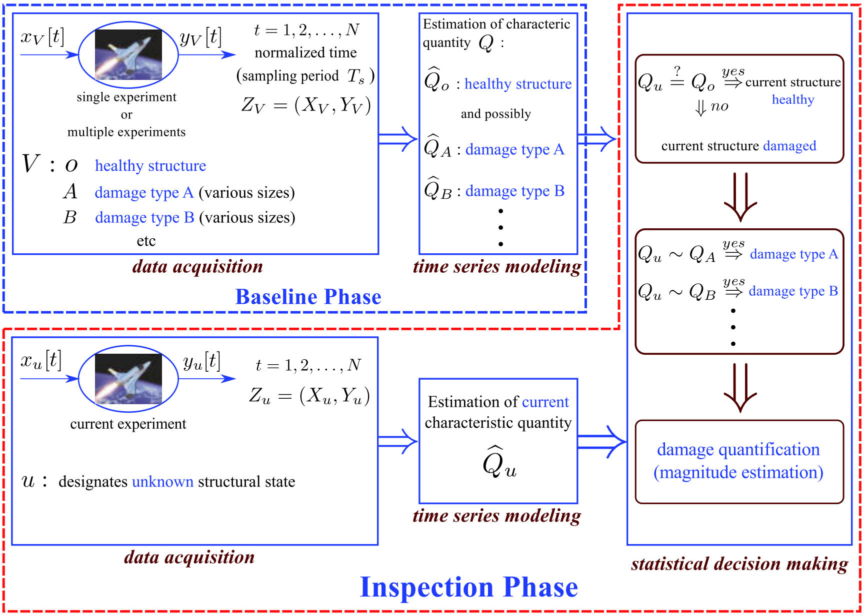

Figure 1. Workframe for statistical time series SHM methods.

2.3 Classes of Statistical Time Series SHM Methods

An important classification of the methods follows the precise nature of the problem in terms of the available signals. *Response-only methods* are based on response signals only, and tackle a generally more difficult problem, while *excitation-response methods* are based on both types of signals. Response-only and excitation-response methods are both treated in sections 4 and 5.

An additional important classification follows the *non-parametric* or *parametric* nature of the statistical time series model used, on which the characteristic quantity Q is based. Non-parametric methods are thus based on corresponding models (see section 3.1), such as non-parametric Power Spectral Density (PSD) or Frequency Response Function (FRF) representations (Söderström and Stoica, 1989; Ljung, 1999; Bendat and Piersol, 2000), and have received limited attention in the literature (Fassois and Sakellariou, 2007, 2009; Kopsaftopoulos and Fassois, 2010, 2011; Benedetti et al., 2011). Parametric methods are likewise based on corresponding models (see section 3.2), such as AutoRegressive Moving Average (ARMA) or State Space (SS) representations (Söderström and Stoica, 1989; Ljung, 1999; Fassois, 2001).

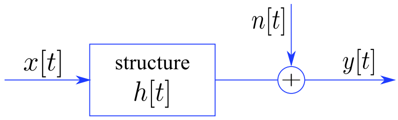

Figure 2. Excitation-response representation of linear time-invariant structural dynamics with additive response noise.

This type of methods has attracted considerable attention and their principles have been used in a number of studies (Fassois and Sakellariou, 2007, 2009; Kopsaftopoulos and Fassois, 2010, 2011). Non-parametric methods offer simplicity and the computational efficiency – selected non-parametric methods are presented in section 4. Parametric methods typically are more elaborate and are characterized by higher computational complexity, but are generally capable of achieving better performance – selected parametric methods are presented in section 5.

Various other classifications are possible, for instance *scalar (univariate)* versus *vector (multivariate)* methods, *time-invariant (stationary)* versus *time-varying (non-stationary)* methods, *linear dynamics* versus *non-linear dynamics* methods, and so forth. Due to space limitations only the scalar, time-invariant and linear dynamics case is treated in this chapter.

3 Statistical Time Series Models of the Structural Dynamics

Statistical time series models for the representation of linear and time-invariant structural dynamics are presented in this section for the univariate (scalar) case. Let $h[t]$ designate the time-discretized impulse response function describing the causality relation between an excitation and vibration response signal, as illustrated in Figure 2. Let $x[t]$ represent the excitation and $y[t]$ the noise-corrupted response signal, with the additive noise $n[t]$ being a stationary Gaussian process, mutually uncorrelated with the excitation, and with zero mean but unknown autocovariance (and thus auto power spectral density).

The excitation and response signals are related through the convolution summation plus noise expression:

$$y[t] = h[t] * x[t] + n[t] = \sum_{\tau=0}^{\infty} h[\tau] \cdot x[t-\tau] + n[t] \tag{1}$$

with $*$ designating discrete convolution. Alternatively, using the backshift operator $\mathcal{B}$ (defined such that[2] $\mathcal{B}^i \cdot y[t] = y[t-i]$), the above may be expressed as:

$$y[t] = H(\mathcal{B}) \cdot x[t] + n[t], \quad \text{with} \quad H(\mathcal{B}) = \sum_{\tau=0}^{\infty} h[\tau] \cdot \mathcal{B}^{\tau} \tag{2}$$

where $H(\mathcal{B})$ stands for the discrete-time structural dynamics transfer function.

3.1 Non-Parametric Models

Assuming that $x[t]$ is a random stationary excitation, then the response $y[t]$ will also be stationary in the steady state. Furthermore, $y[t]$ will be Gaussian if $x[t]$ and $n[t]$ are jointly Gaussian. In this case each signal is fully characterized by its first two moments, *mean* and *AutoCovariance Function (ACF)*. Instead of the autocovariance function $\gamma_{yy}[\tau]$ (or its normalized version $\rho_{yy}[\tau]$), its Fourier transform which is the *auto Power Spectral Density (PSD)* $S_{yy}(\omega)$ (Kay 1988, p. 3, Box et al. 1994, pp. 39–40) may be employed. Thus:

$$\mu_y = E\{y[t]\} \tag{3}$$

$$\gamma_{yy}[\tau] = E\{\tilde{y}[t] \cdot \tilde{y}[t-\tau]\} \tag{4}$$

$$\rho_{yy}[\tau] = \frac{\gamma_{yy}[\tau]}{\gamma_{yy}[0]} \in [-1, 1] \tag{5}$$

$$S_{yy}(\omega) = \sum_{\tau=-\infty}^{\infty} \gamma_{yy}[\tau] \cdot e^{-j\omega\tau T_s}. \tag{6}$$

In these expressions $E\{\cdot\}$ designates statistical expectation, j the imaginary unit, τ time lag, $\omega \in [0, 2\pi/T_s]$ frequency (rad/s), T_s the sampling period, and $\tilde{y}[t] = y[t] - \mu_y$. Moreover, note that $\gamma_{yy}[0]$ is equal to the variance σ_y^2 of the response $y[t]$. The first order moment, along with any suitable form of the second order moment, constitute a *response-only* time series model (summary in Table 3).

In the *excitation-response* case, a complete joint description of the excitation and response signals is given in terms of the means μ_x and μ_y, and the ACFs $\gamma_{xx}[\tau]$, $\gamma_{yy}[\tau]$ and *Cross Covariance Function (CCF)* $\gamma_{yx}[\tau]$ (or their normalized equivalents). An equivalent representation may be obtained by using the auto PSDs $S_{xx}(\omega)$, $S_{yy}(\omega)$ and *Cross Spectral Density (CSD)* $S_{yx}(j\omega)$.

[2]The backshift operator is alternatively designated as q^{-1}, or as z^{-1} in the z domain – yet the designation $\mathcal{B}$ is exclusively used in this chapter.

Table 3. The elements of non-parametric response-only models.

Mean:	$\mu_y = E\{y[t]\}$
ACF:	$\gamma_{yy}[\tau] = E\{\tilde{y}[t] \cdot \tilde{y}[t-\tau]\}$
normalized ACF:	$\rho_{yy}[\tau] = \gamma_{yy}[\tau]/\gamma_{yy}[0] \ \in [-1, 1]$
auto PSD:	$S_{yy}(\omega) = \sum_{\tau=-\infty}^{\infty} \gamma_{yy}[\tau] \cdot e^{-j\omega\tau T_s}$

$\tilde{y}[t] = y[t] - \mu_y$

The response characteristics are related to those of the excitation and the noise through the expressions (Box et al., 1994, pp. 455–456):

$$\mu_y = H(j\omega)|_{\omega=0} \cdot \mu_x \tag{7a}$$

$$\gamma_{yx}[\tau] = \gamma_{xx}[\tau] * h[\tau] \tag{7b}$$

$$\gamma_{yy}[\tau] = \gamma_{yx}[\tau] * h[-\tau] + \gamma_{nn}[\tau] \tag{7c}$$

$$S_{yx}(j\omega) = H(j\omega) \cdot S_{xx}(\omega) \tag{8a}$$

$$S_{yy}(\omega) = H^\star(j\omega) \cdot S_{yx}(j\omega) + S_{nn}(\omega) = |H(j\omega)|^2 \cdot S_{xx}(\omega) + S_{nn}(\omega) \tag{8b}$$

with $*$ designating discrete convolution, the superscript $\star$ complex conjugation, and $|\cdot|$ complex magnitude. $H(j\omega) = H(\mathcal{B})|_{\mathcal{B}=e^{-j\omega T_s}}$ designates the structural *Frequency Response Function (FRF)*, $S_{nn}(\omega)$ the noise auto PSD, and $S_{yx}(j\omega)$ the CSD between the designated signals defined as the Fourier transform of the corresponding CCF.

In addition, the squared *coherence function* is defined as (Bendat and Piersol, 2000, p. 196):

$$\gamma^2(\omega) = \frac{|S_{yx}(j\omega)|^2}{S_{xx}(\omega) \cdot S_{yy}(\omega)} = \frac{1}{1 + \frac{S_{nn}(\omega)}{|H(j\omega)|^2 \cdot S_{xx}(\omega)}} \ \in \ [0, 1]. \tag{9}$$

The elements of non-parametric excitation-response time series models are summarized in Table 4.

3.2 Parametric Models

Parametric time series models may be obtained via proper parametrizations of Equation (1). In the response-only case it is assumed, without loss of generality, that the excitation is white (uncorrelated), that is $\gamma_{xx}[\tau] = 0$ for $\tau \neq 0$, in which case the signal is often designated as $w[t]$, while $n[t] \equiv 0$. Moreover, the signals are assumed zero mean, thus $\tilde{y}[t] = y[t] - \mu_y$ is typically used.

Table 4. The elements of non-parametric excitation-response models.

Means:	μ_x	μ_y
ACFs:	$\gamma_{xx}[\tau]$	$\gamma_{yy}[\tau]$
normalized ACFs:	$\rho_{xx}[\tau]$	$\rho_{yy}[\tau]$
CCF:	$\gamma_{yx}[\tau] = E\{\tilde{y}[t] \cdot \tilde{x}[t-\tau]\}$	
normalized CCF:	$\rho_{yx}[\tau] = \gamma_{yx}[\tau] / \sqrt{\gamma_{xx}[0] \cdot \gamma_{yy}[0]} \ \in [-1, 1]$	
auto PSDs:	$S_{xx}(\omega)$	$S_{yy}(\omega)$
CSD:	$S_{yx}(j\omega) = \sum_{\tau=-\infty}^{\infty} \gamma_{yx}[\tau] \cdot e^{-j\omega\tau T_s}$	

$\tilde{x}[t] = x[t] - \mu_x$, $\tilde{y}[t] = y[t] - \mu_y$

The parametrization of Equation (1) in the response-only case leads to the celebrated *AutoRegressive Moving Average (ARMA)* model (Box et al., 1994, pp. 52–53):

$$y[t] + \sum_{i=1}^{na} a_i \cdot y[t-i] = w[t] + \sum_{i=1}^{nc} c_i \cdot w[t-i] \tag{10a}$$

which, using the backshift operator, is also written as:

$$\begin{aligned} &\left(1 + \sum_{i=1}^{na} a_i \cdot \mathcal{B}^i\right) \cdot y[t] = \left(1 + \sum_{i=1}^{nc} c_i \cdot \mathcal{B}^i\right) \cdot w[t] \Longleftrightarrow \\ &\Longleftrightarrow A(\mathcal{B}) \cdot y[t] = C(\mathcal{B}) \cdot w[t], \quad w[t] \sim \text{iid}\, \mathcal{N}(0, \sigma_w^2) \end{aligned} \tag{10b}$$

with a_i, c_i, $A(\mathcal{B})$, and $C(\mathcal{B})$ designating the AR and MA parameters and corresponding polynomials, respectively, iid stands for identically independently distributed, $\mathcal{N}(\cdot,\cdot)$ designates normal distribution with the indicated mean and variance, while na, nc are the model's AR, MA orders, respectively. The model parameter vector is $\boldsymbol{\theta} = [\text{coef}(A)\ \text{coef}(B)]^T$. It should be noted that $w[t]$ coincides with the *one-step-ahead-prediction error* and is also referred to as the *model residual* or *innovations* (Box et al. 1994, p. 134, Ljung 1999, p. 70). Corresponding *Vector AutoRegressive Moving Average (VARMA)* models are available for the multivariate case (see Söderström and Stoica, 1989; Lütkepohl, 2005).

The ARMA representation of Equations (10a) – (10b) may be equivalently set into *State Space (SS)* form, consisting of a first order state equation plus an output equation (Söderström and Stoica 1989, p. 157, Box et al. 1994, pp. 163–164):

$$\boldsymbol{\psi}[t+1] = \boldsymbol{A} \cdot \boldsymbol{\psi}[t] + \boldsymbol{K} \cdot \boldsymbol{v}[t], \quad \boldsymbol{v}[t] \sim \text{iid}\, \mathcal{N}(\mathbf{0}, \boldsymbol{\Sigma}_{\boldsymbol{v}}) \tag{11a}$$

$$y[t] = \boldsymbol{C} \cdot \boldsymbol{\psi}[t] + \boldsymbol{v}[t] \tag{11b}$$

Table 5. Parametric response-only models.

ARMA:	$A(\mathcal{B}) \cdot y[t] = C(\mathcal{B}) \cdot w[t]$	$A(\mathcal{B}) = 1 + \sum_{i=1}^{na} a_i \mathcal{B}^i$
		$C(\mathcal{B}) = 1 + \sum_{i=1}^{nc} c_i \mathcal{B}^i$
	$w[t] \sim \text{iid}\, \mathcal{N}(0, \sigma_w^2)$	na, nc : AR, MA orders
State Space (SS):	$\boldsymbol{\psi}[t+1] = \boldsymbol{A} \cdot \boldsymbol{\psi}[t] + \boldsymbol{K} \cdot \boldsymbol{v}[t]$	$\boldsymbol{\psi}[t]$: state vector
	$y[t] = \boldsymbol{C} \cdot \boldsymbol{\psi}[t] + \boldsymbol{v}[t]$	$\boldsymbol{v}[t] \sim \text{iid}\, \mathcal{N}(\mathbf{0}, \boldsymbol{\Sigma}_v)$
		$\boldsymbol{A}$: system matrix
		$\boldsymbol{C}$: output matrix
		$\boldsymbol{K}$: Kalman gain matrix

with $\boldsymbol{\psi}[t]$ designating the model's state vector and $\boldsymbol{v}[t]$ a zero mean uncorrelated (white) vector sequence with covariance $\boldsymbol{\Sigma_v}$. $\boldsymbol{A}$, $\boldsymbol{C}$, $\boldsymbol{K}$ designate proper matrices and the parameter vector is $\boldsymbol{\theta} = [\text{vec}(\boldsymbol{A})\ \text{vec}(\boldsymbol{C})\ \text{vec}(\boldsymbol{K})]$, with vec$(\cdot)$ designating the column vector operator. These parametric response-only time series models are summarized in Table 5.

In the excitation-response case different parametrizations of Equation (1) lead to different models. The simplest one is the *AutoRegressive with eXogenous excitation (ARX)* model (Söderström and Stoica 1989, pp. 149–151, Ljung 1999, p. 81, Fassois 2001):

$$y[t] + \sum_{i=1}^{na} a_i \cdot y[t-i] = \sum_{i=0}^{nb} b_i \cdot x[t-i] + w[t] \tag{12a}$$

or using the backshift operator:

$$A(\mathcal{B}) \cdot y[t] = B(\mathcal{B}) \cdot x[t] + w[t] \quad \Longleftrightarrow$$

$$\Longleftrightarrow \quad y[t] = \frac{B(\mathcal{B})}{A(\mathcal{B})} \cdot x[t] + \frac{1}{A(\mathcal{B})} \cdot w[t], \quad w[t] \sim \text{iid}\, \mathcal{N}(0, \sigma_w^2) \tag{12b}$$

with $A(\mathcal{B})$ and $B(\mathcal{B})$ designating the AR and X polynomials, respectively, and na, nb the corresponding orders. The parameter vector is defined as $\boldsymbol{\theta} = [\text{coef}(A)\ \text{coef}(B)]^T$, while $w[t]$ is a zero mean, uncorrelated (white) signal, which coincides with the model based one-step-ahead prediction error. In the special case of $na = 0$, a Finite Impulse Response (FIR) model is obtained. The ARX model block diagram is depicted in Figure 3.

A more general and flexible representation is the *AutoRegressive Moving Average with eXogenous excitation (ARMAX)*, which additionally involves a Moving Average (MA) polynomial $C(\mathcal{B})$ for describing the noise dynamics

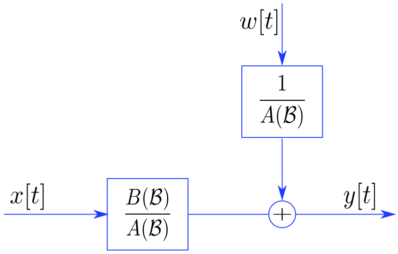

Figure 3. The ARX model structure.

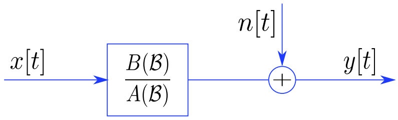

Figure 4. The Output Error (OE) model structure.

(Söderström and Stoica 1989, pp. 149–151, Ljung 1999, p. 83, Fassois 2001):

$$y[t] + \sum_{i=1}^{na} a_i \cdot y[t-i] = \sum_{i=0}^{nb} b_i \cdot x[t-i] + w[t] + \sum_{i=1}^{nc} c_i \cdot w[t-i] \tag{13a}$$

or using the backshift operator:

$$A(\mathcal{B}) \cdot y[t] = B(\mathcal{B}) \cdot x[t] + C(\mathcal{B}) \cdot w[t] \quad \Longleftrightarrow$$

$$\Longleftrightarrow \quad y[t] = \frac{B(\mathcal{B})}{A(\mathcal{B})} \cdot x[t] + \frac{C(\mathcal{B})}{A(\mathcal{B})} \cdot w[t], \quad w[t] \sim \text{iid}\, \mathcal{N}(0, \sigma_w^2) \tag{13b}$$

with nc designating the MA order. The parameter vector is defined as $\boldsymbol{\theta} = [\text{coef}(A)\ \text{coef}(B)\ \text{coef}(C)]^T$.

The *Output Error (OE)* representation models the excitation-response dynamics while avoiding noise modelling (Söderström and Stoica 1989, p. 153, Ljung 1999, p. 85, Fassois 2001):

$$y[t] = \frac{B(\mathcal{B})}{A(\mathcal{B})} \cdot x[t] + n[t]. \tag{14}$$

The parameter vector in this case is $\boldsymbol{\theta} = [\text{coef}(A)\ \text{coef}(B)]^T$ and the model's block diagram is depicted in Figure 4.

Table 6. Parametric excitation-response models.

ARX:	$A(\mathcal{B}) \cdot y[t] = B(\mathcal{B}) \cdot x[t] + w[t]$	na, nb : AR, X orders $A(\mathcal{B}) = 1 + \sum_{i=1}^{na} a_i \mathcal{B}^i$ $B(\mathcal{B}) = b_0 + \sum_{i=1}^{nb} b_i \mathcal{B}^i$
ARMAX:	$A(\mathcal{B}) \cdot y[t] = B(\mathcal{B}) \cdot x[t] + C(\mathcal{B}) \cdot w[t]$	nc : MA order $C(\mathcal{B}) = 1 + \sum_{i=1}^{nc} c_i \mathcal{B}^i$
Output Error:	$y[t] = \frac{B(\mathcal{B})}{A(\mathcal{B})} \cdot x[t] + n[t]$	$n[t]$: autocorrelated zero mean
Box-Jenkins:	$y[t] = \frac{B(\mathcal{B})}{A(\mathcal{B})} \cdot x[t] + \frac{C(\mathcal{B})}{D(\mathcal{B})} \cdot w[t]$	$D(\mathcal{B}) = 1 + \sum_{i=1}^{nd} d_i \mathcal{B}^i$
State Space:	$\boldsymbol{\psi}[t+1] = \boldsymbol{A} \cdot \boldsymbol{\psi}[t] + \boldsymbol{B} \cdot x[t] + \boldsymbol{K} \cdot \boldsymbol{v}[t]$ $y[t] = \boldsymbol{C} \cdot \boldsymbol{\psi}[t] + \boldsymbol{D} \cdot x[t] + \boldsymbol{v}[t]$	$\boldsymbol{\psi}[t]$: state vector $\boldsymbol{v}[t] \sim \text{iid}\, \mathcal{N}(\mathbf{0}, \boldsymbol{\Sigma}_v)$
	$\boldsymbol{A}$: system matrix, $\boldsymbol{B}$: input matrix, $\boldsymbol{K}$: Kalman gain matrix	
	$\boldsymbol{C}$: output matrix, $\boldsymbol{D}$: dir. transm. matrix	

$w[t] \sim \text{iid}\, \mathcal{N}(0, \sigma_w^2)$

Alternatively, the *Box-Jenkins (BJ)* representation independently models the structural and noise dynamics (Söderström and Stoica 1989, pp. 148–154, Ljung 1999, p. 87):

$$y[t] = \frac{B(\mathcal{B})}{A(\mathcal{B})} \cdot x[t] + \frac{C(\mathcal{B})}{D(\mathcal{B})} \cdot w[t], \quad w[t] \sim \text{iid}\, \mathcal{N}(0, \sigma_w^2) \tag{15}$$

with parameter vector $\boldsymbol{\theta} = [\text{coef}(A)\ \text{coef}(B)\ \text{coef}(C)\ \text{coef}(D)]^T$.

Finally, a State Space (SS) representation in this case assumes the form (Ljung, 1999, pp. 97–101)):

$$\boldsymbol{\psi}[t+1] = \boldsymbol{A} \cdot \boldsymbol{\psi}[t] + \boldsymbol{B} \cdot x[t] + \boldsymbol{K} \cdot \boldsymbol{v}[t], \ \boldsymbol{v}[t] \sim \text{iid}\, \mathcal{N}(\mathbf{0}, \boldsymbol{\Sigma_v}) \tag{16a}$$

$$y[t] = \boldsymbol{C} \cdot \boldsymbol{\psi}[t] + \boldsymbol{D} \cdot x[t] + \boldsymbol{v}[t] \tag{16b}$$

with $\boldsymbol{\psi}[t]$ designating the model's state vector and $\boldsymbol{v}[t]$ a zero mean uncorrelated (white) vector sequence with covariance $\boldsymbol{\Sigma_v}$ and the model parameter vector being $\boldsymbol{\theta} = [\text{vec}(\boldsymbol{A})\ \text{vec}(\boldsymbol{B})\ \text{vec}(\boldsymbol{C})\ \text{vec}(\boldsymbol{D})\ \text{vec}(\boldsymbol{K})]$. The parametric excitation-response time series models are summarized in Table 6.

3.3 Identification of Time Series Models

Model identification refers to the estimation of statistical time series models based on excitation $x[t]$ and/or response $y[t]$ random vibration data records (for $t = 1, 2, \ldots, N$) that are properly preprocessed and are collectively designated as $Z = (X, Y)$. This is achieved via *estimators*, which operate on the obtained data records to provide *estimates* of the quantities of interest.

The estimator of a quantity Q is designated as $\widehat{Q}$ and is a function of the random data Z, thus $\widehat{Q} = g(Z)$. Viewing each data point as the realization (observed value) of an underlying random variable, the estimator is a function of several random variables, and thus a random variable as well with probability density function (pdf) $f_{\widehat{Q}}$. For Gaussian distribution this is expressed as $\widehat{Q} \sim \mathcal{N}(\mu_{\widehat{Q}}, \mathrm{var}[\widehat{Q}])$, with the arguments $\mu_{\widehat{Q}}$ and $\mathrm{var}[\widehat{Q}]$ designating the estimator mean and variance, respectively.

Estimators may be characterized by several important properties. One of them is unbiasedness, implying that its mean $\mu_{\widehat{Q}}$ coincides with the true value of the quantity being estimated, that is $E\{\widehat{Q}\} = Q$; when this is true the estimator is referred to as *unbiased*. Oftentimes, unbiasedness or other estimator properties (such as Gaussianity or minimum variance which is referred to as *efficiency*) are only valid *asymptotically*, as the data record length (in samples) tends to infinity ($N \to \infty$). Some other properties such as *consistency* by definition refer to the estimator asymptotic behaviour in a proper sense ($\lim_{N\to\infty} \widehat{Q}(N) \to Q$). Certain properties of non-parametric statistical time series estimators are summarized in Table 7.

The identification of parametric time series models is divided into two main tasks: parameter estimation and model structure selection. Typical methods for parameter estimation include the Least Squares (LS), the Prediction Error (PE), the Maximum Likelihood (ML), and subspace methods (Söderström and Stoica 1989, Chapters 7–8, Ljung 1999, Chapter 7).

Model structure selection, which refers to the determination of the model orders, is generally a more complicated procedure and is typically achieved by identifying increasingly higher order models until no further "improvement" is observed. "Improvement" may be judged via a variety of criteria, such as the model Residual Sum of Squares (RSS – often normalized by the Signal Sum of Squares, SSS), or the negative likelihood, or those criteria that include a penalty term for high model dimensionality, such as the Akaike Information Criterion (AIC) and the Bayesian Information Criterion (BIC) (Söderström and Stoica 1989, pp. 442–443, Ljung 1999, pp. 505–507, Fassois 2001). Other "practical" criteria, such as PSD or FRF or modal frequency stabilization diagrams are also used (Fassois, 2001). In all cases it is advised to simultaneously monitor the Signal Per (estimated) Parameter (SPP) ratio which must be maintained sufficiently high (say above 15), as well as the numerical accuracy (for instance by monitoring the condition

Table 7. Estimation of non-parametric statistical time series model characteristics.

Quantity	Power Spectral Density (PSD)	Frequency Response Function (FRF)
Estimator	$\widehat{S}_{yy}(\omega) = \frac{1}{K}\sum_{i=1}^{K}\widehat{Y}_L^i(j\omega)\widehat{Y}_L^i(-j\omega)$ $\widehat{Y}_L^i(j\omega) = \frac{1}{\sqrt{L}}\sum_{t=1}^{L}a[t]\widehat{y}^i[t]e^{-j\omega T_s}$ $\widehat{y}^i[t] = y^i[t] - \widehat{\mu}_y$ (i-th segment of length L)	$\widehat{H}(j\omega) = \widehat{S}_{yx}(j\omega)/\widehat{S}_{xx}(\omega)$
Properties	$2K\widehat{S}_{yy}(\omega)/S_{yy}(\omega) \sim \chi^2(2K)$	$E\{\lvert\widehat{H}(j\omega)\rvert\} \approx \lvert H(j\omega)\rvert$ $\mathrm{var}[\lvert\widehat{H}(j\omega)\rvert] \approx \frac{1-\gamma^2(\omega)}{\gamma^2(\omega)2K}\lvert H(j\omega)\rvert^2$
Comments	Welch method (no overlap) K : number of data segments $a[t]$: time window	For $N \to \infty$, $a[t] = 1$ $\gamma^2(\omega) \to 1$ or $K \to \infty$

Remarks:
$\omega \in [0, 2\pi/T_s]$ stands for frequency (rad/s); j stands for the imaginary unit.
K stands for the number of segments used in Welch spectral estimation.
$\gamma^2(\omega)$ stands for the coherence function (Bendat and Piersol, 2000, p. 196).
The FRF magnitude estimator distribution may be approximated as Gaussian for small relative errors (Bendat and Piersol, 2000, pp. 274–275).
MATLAB functions: *pwelch.m* for $\widehat{S}_{yy}$, *tfestimate.m* for $\widehat{H}$.

number of the matrices inverted during estimation).

4 Selected Non-Parametric Time Series SHM Methods

Non-parametric methods are those in which the characteristic quantity Q is constructed based on non-parametric time series models (Tables 3 and 4). A response-only *Power Spectral Density (PSD)* method and an excitation-response *Frequency Response Function (FRF)* method are outlined in the sequel. For alternative methods that employ a novelty measure see Worden (1997); Worden et al. (2000); Worden and Manson (2003); Manson et al. (2003).

4.1 PSD Based Method

This method tackles damage detection and identification via changes in the auto Power Spectral Density (PSD) of the measured vibration response signal when the excitation is not available (response-only case). The method's characteristic quantity thus is $Q = S_{yy}(\omega) = S(\omega)$. The main idea is based on the comparison of the current structure's response PSD, $S_u(\omega)$, to that of the healthy structure's, $S_o(\omega)$ (or, in fact, to that corresponding to any other structural state). The response signals must be normalized in order to properly account for potentially different levels of excitation.

Damage detection is based on the following hypothesis testing problem:

$$\begin{aligned} &H_o:\ S_u(\omega) = S_o(\omega) \text{ (null hypothesis – healthy structure)} \\ &H_1:\ S_u(\omega) \neq S_o(\omega) \text{ (alternative hypothesis – damaged structure).} \end{aligned} \tag{17}$$

As the true PSDs, $S_u(\omega)$ and $S_o(\omega)$, are unknown, their estimates, $\widehat{S}_u(\omega)$ and $\widehat{S}_o(\omega)$, obtained via the Welch method (with K non-overlapping segments; refer to Table 7) are used (Kay, 1988, pp. 3 and 76). Then, the quantity F, below, follows $\mathcal{F}$ distribution with $(2K, 2K)$ degrees of freedom for each frequency ω (as the ratio of two random variables each following a normalized χ^2 distribution with $2K$ degrees of freedom; see Appendix):

$$F = \frac{\widehat{S}_o(\omega)/S_o(\omega)}{\widehat{S}_u(\omega)/S_u(\omega)} \sim \mathcal{F}(2K, 2K). \tag{18}$$

Under the null hypothesis H_o of a healthy structure, the true PSDs coincide, $S_u(\omega) = S_o(\omega)$, thus:

$$\text{Under } H_o: \quad F = \frac{\widehat{S}_o(\omega)}{\widehat{S}_u(\omega)} \sim \mathcal{F}(2K, 2K). \tag{19}$$

Then F should be in the range $[f_{\alpha/2}, f_{1-\alpha/2}]$ with probability $1-\alpha$, and decision making is as follows for a selected α (false alarm) risk level – see Figure 5:

$$\begin{aligned} &f_{\frac{\alpha}{2}}(2K, 2K) \leq F \leq f_{1-\frac{\alpha}{2}}(2K, 2K) \quad (\forall\, \omega) \\ &\qquad \Longrightarrow H_o \text{ is accepted} \quad \text{(healthy structure)} \\ &\text{Else} \quad \Longrightarrow H_1 \text{ is accepted} \quad \text{(damaged structure),} \end{aligned} \tag{20}$$

with $f_{\alpha/2}, f_{1-\alpha/2}$ designating the $\mathcal{F}$ distribution's $\alpha/2$ and $1-(\alpha/2)$ critical points (f_α is defined such that $\text{Prob}(F \leq f_\alpha) = \alpha$).

Damage identification may be achieved by performing hypotheses testing similar to the above for damages from each potential damage type (see Table 2). Damage quantification may be achieved by possibly associating specific quantitative changes in the PSD with specific damage magnitudes.

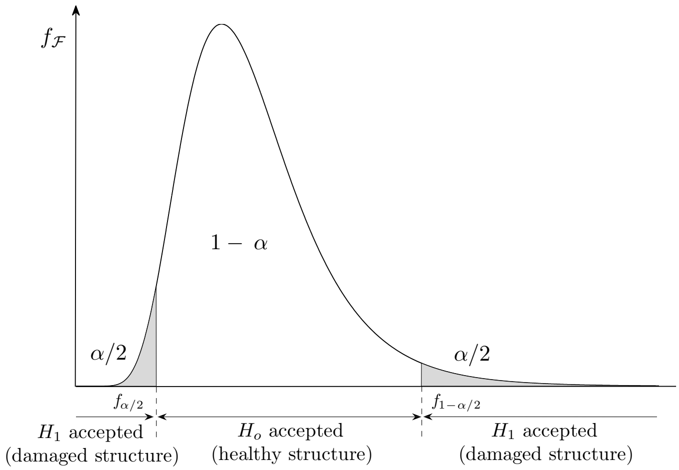

Figure 5. Statistical hypothesis testing based on an $\mathcal{F}$ distributed statistic (two-tail test).

Bibliographical remarks. Sakellariou et al. (2001) present the application of a variant of the PSD based method to fault detection on a railway vehicle suspension. Liberatore and Carman (2004) present the application of a simplified version (not using a statistical framework) to a simply supported aluminum beam. In the non-stationary or non-linear cases, time-frequency, polyspectra, or wavelet-based models may be used (Farrar and Doebling, 1997; Staszewski, 1998, 2000; Hou et al., 2000; Hera and Hou, 2004; Peng and Chu, 2004; Staszewski and Robertson, 2007).

4.2 FRF Magnitude Based Method

The FRF magnitude based method is similar to the PSD based method, but refers to the the excitation-response case and employs the FRF magnitude as the characteristic quantity $Q = |H(j\omega)|$. A somewhat similar approach may be used in case the excitation is unavailable but several responses are available (Sakellariou and Fassois, 2006; Mao and Todd, 2011). The main idea is the comparison of the FRF magnitude $|H_u(j\omega)|$ of the current state of the structure to that of the healthy structure $|H_o(j\omega)|$ (or, in fact, to that corresponding to any other structural state).

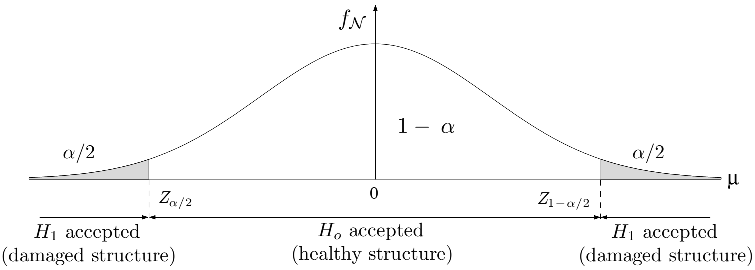

Figure 6. Statistical hypothesis testing based on a Gaussian distributed statistic (two-tail test).

Damage detection is based on the following hypothesis testing problem:

$$\begin{array}{ll} H_o: & \delta|H(j\omega)| = |H_o(j\omega)| - |H_u(j\omega)| = 0 \\ \multicolumn{2}{l}{\text{(null hypothesis – healthy structure)}} \\ H_1: & \delta|H(j\omega)| = |H_o(j\omega)| - |H_u(j\omega)| \neq 0 \\ \multicolumn{2}{l}{\text{(alternative hypothesis – damaged structure).}} \end{array} \tag{21}$$

As the true FRFs $H_u(j\omega)$ and $H_o(j\omega)$ are unknown, their corresponding estimates, $\widehat{H}_u(j\omega)$ and $\widehat{H}_o(j\omega)$, obtained as indicated in Table 7, are employed. As indicated there, the FRF magnitude estimator may, asymptotically ($N \to \infty$), be considered to approximately follow Gaussian distribution (Bendat and Piersol, 2000, p. 338). As the data records Z_u and Z_o are mutually independent, the two FRF magnitude estimators are also mutually independent, implying that their difference $|\widehat{H}_o(j\omega)| - |\widehat{H}_u(j\omega)|$ is Gaussian with mean equal to the true magnitude difference and variance equal to the sum of the two variances.

Under the null hypothesis H_o (healthy structure), the true FRF magnitudes coincide ($|H_u(j\omega)| = |H_o(j\omega)|$), hence:

$$\text{Under } H_o: \quad \delta|\widehat{H}(j\omega)| = |\widehat{H}_o(j\omega)| - |\widehat{H}_u(j\omega)| \sim \mathcal{N}(0, 2\sigma_o^2(\omega)). \tag{22}$$

The variance $\sigma_o^2(\omega) = \mathrm{var}[|\widehat{H}_o(j\omega)|]$ is generally unknown, but may be estimated in the baseline phase (Table 7). Assuming negligible variability of this estimate (which is true for "large" N), equality of the two FRF magnitudes may be examined at the selected α (false alarm) risk level through the following statistical test (Figure 6):

$$\begin{array}{lll} Z = \big|\delta|\widehat{H}(j\omega)|\big| / \sqrt{2\widehat{\sigma}_o^2(\omega)} \le Z_{1-\frac{\alpha}{2}} \quad (\forall\, \omega) & \Longrightarrow H_o \text{ is accepted} \\ \qquad\qquad\qquad \text{Else} & \Longrightarrow H_1 \text{ is accepted,} \end{array} \tag{23}$$

with $Z_{1-\alpha/2}$ designating the standard normal distribution's $1-\alpha/2$ critical point.

Damage identification may be similarly achieved by performing hypotheses testing similar to the above for damages from each potential damage type (see Table 2). Damage quantification may be achieved by possibly associating specific quantitative changes in the FRF magnitude with specific damage magnitudes.

Bibliographical remarks. Hwang and Kim (2004) present an FRF based method (though not in a statistical context), whose effectiveness is numerically demonstrated via simulation examples based on Finite Element (FE) models of a simple cantilever and a helicopter rotor blade. The method is reported to achieve satisfactory damage diagnosis. Rizos et al. (2008) employ the method for skin damage detection in stiffened aircraft panels. Changes in the FRF magnitude estimates due to damage are shown to exceed their normal variability bounds.

5 Selected Parametric Time Series SHM Methods

Parametric time series methods are those in which the characteristic quantity Q is constructed based on parametric time series representations. The response-only or excitation-response cases may be dealt with through the use of corresponding models (Basseville and Nikiforov 1993, section 6.2, Natke and Cempel 1997, Gertler 1998, section 4.2). Although parametric methods may operate on either the time or frequency domains, the former case is more widely used and is in the focus of this section.

Parametric methods may be further classified into three main categories:

(i) *Model parameter based methods*, which tackle damage detection and identification via a characteristic quantity Q that is a function of the estimated model parameters. These methods require that a model is re-estimated during the inspection phase based on the current signals Z_u.

(ii) *Model residual based methods*, which tackle damage detection and identification via characteristic quantities Q that are functions of the model residuals generated by driving the current signals Z_u through predetermined, in the baseline phase, models corresponding to the considered structural states. An advantage of these methods is that no model re-estimation is required in the inspection phase.

(iii) *Functional model (FM) based methods* constitute a family of advanced schemes which are capable of properly treating the subproblems of damage detection, identification (localization) and magnitude estimation within a unified framework. Damages characterized by a *double continuum* of locations and magnitudes on a structural topology may be considered. Model estimation is required in the inspection phase.

5.1 Model Parameter Based Methods

These methods perform damage detection and identification based on a characteristic quantity $Q = f(\boldsymbol{\theta})$, which is a function of the parameter vector $\boldsymbol{\theta}$ of a parametric time series model ($Q = \boldsymbol{\theta}$ in the typical case). Transformed forms of the parameter vector $\boldsymbol{\theta}$ may be also used, with the most common and historically important case being that in which the vector of the model natural frequencies is employed (Doebling et al., 1996; Salawu, 1997; Sohn et al., 2003a; Uhl and Mendrok, 2004; Rizos et al., 2008; Hios and Fassois, 2009b).

Let $\widehat{\boldsymbol{\theta}}$ designate a proper estimator of the parameter vector $\boldsymbol{\theta}$ (Söderström and Stoica, 1989, pp. 198–199, Ljung, 1999, pp. 212–213). For sufficiently long signals ("large" N) the estimator is (under mild assumptions) Gaussian distributed with mean equal to its true value $\boldsymbol{\theta}$ and a certain covariance $\boldsymbol{P}_{\boldsymbol{\theta}}$ (Söderström and Stoica, 1989, pp. 205–207, Ljung, 1999, p. 303), that is:

$$\widehat{\boldsymbol{\theta}} \sim \mathcal{N}(\boldsymbol{\theta}, \boldsymbol{P}_{\boldsymbol{\theta}}). \tag{24}$$

Damage detection is based on testing for statistically significant changes in $\boldsymbol{\theta}$ between the nominal and current structural states through the hypothesis testing problem:

$$\begin{array}{l} H_o : \delta\boldsymbol{\theta} = \boldsymbol{\theta}_o - \boldsymbol{\theta}_u = \mathbf{0} \\ \text{(null hypothesis – healthy structure)} \\ H_1 : \delta\boldsymbol{\theta} = \boldsymbol{\theta}_o - \boldsymbol{\theta}_u \neq \mathbf{0} \\ \text{(alternative hypothesis – damaged structure).} \end{array} \tag{25}$$

Due to the mutual independence of the Z_u and Z_o data records, the difference between the two parameter vector estimators also follows Gaussian distribution:

$$\delta\widehat{\boldsymbol{\theta}} = \widehat{\boldsymbol{\theta}}_o - \widehat{\boldsymbol{\theta}}_u \sim \mathcal{N}(\delta\boldsymbol{\theta}, \delta\boldsymbol{P}) \tag{26}$$

with

$$\delta\boldsymbol{\theta} = \boldsymbol{\theta}_o - \boldsymbol{\theta}_u, \quad \delta\boldsymbol{P} = \boldsymbol{P}_o + \boldsymbol{P}_u, \tag{27}$$

where $\boldsymbol{P}_o, \boldsymbol{P}_u$ designate the corresponding covariance matrices.

Under the null (H_o) hypothesis, $\delta\widehat{\boldsymbol{\theta}} = \widehat{\boldsymbol{\theta}}_o - \widehat{\boldsymbol{\theta}}_u \sim \mathcal{N}(\mathbf{0}, 2\boldsymbol{P}_o)$ and the quantity $\chi^2_{\boldsymbol{\theta}}$, below, follows χ^2 distribution with d (parameter vector dimensionality) degrees of freedom (as the sum of squares of independent standardized Gaussian variables – see Ljung 1999, p. 558 and Appendix):

$$\text{Under } H_o: \quad \chi^2_{\boldsymbol{\theta}} = \delta\widehat{\boldsymbol{\theta}}^T \cdot \delta\boldsymbol{P}^{-1} \cdot \delta\widehat{\boldsymbol{\theta}} \sim \chi^2(d) \tag{28}$$

with $\delta\boldsymbol{P} = 2\boldsymbol{P}_o$.

As the covariance matrix $\boldsymbol{P}_o$ corresponding to the healthy structure is unavailable, the estimated covariance $\widehat{\boldsymbol{P}}_o$ is used. Treating this as a quantity characterized by negligible variability (reasonable for large N), leads to the following test constructed at the α (false alarm) risk level (Figure 7):

$$\begin{array}{lcll} \chi^2_{\boldsymbol{\theta}} \leq \chi^2_{1-\alpha}(d) & \Longrightarrow & H_o \text{ is accepted} & \text{(healthy structure)} \\ \text{Else} & \Longrightarrow & H_1 \text{ is accepted} & \text{(damaged structure)}, \end{array} \tag{29}$$

with $\chi^2_{1-\alpha}(d)$ designating the χ^2 distribution's $1-\alpha$ critical point. See Ljung 1999, p. 559 for an alternative approach based on the $\mathcal{F}$ distribution.

Damage identification may be based on the multiple hypotheses testing problem of Table 2 comparing the parameter vector $\widehat{\boldsymbol{\theta}}_u$ belonging to the current state of the structure to those corresponding to different damage types $\widehat{\boldsymbol{\theta}}_A, \widehat{\boldsymbol{\theta}}_B, \ldots$. Nevertheless, this is expected to work only for damages of specific magnitudes and cannot generally account for the continuum of damage magnitudes within each damage type. A *geometric method* aiming at circumventing this difficulty and also being suitable for damage estimation is presented in Sakellariou and Fassois (2006). Essentially this is a predecessor of Functional Model (FM) based methods and the reader is directed to subsection 5.3.

Bibliographical remarks. The principles of the model parameter based methods have been used in a number of studies. Sohn and Farrar (2000) use the parameters of an AR model and statistical process control charts for damage detection in a concrete bridge column, as it is progressively damaged. Adams and Farrar (2002) use frequency domain ARX models for damage detection in a simulated structural system and a three-story building model. Nair et al. (2006) employ the first three autoregressive parameters of an ARMA model to tackle damage detection. The postulated method is applied to analytical and experimental data from the ASCE benchmark structure. Sakellariou and Fassois (2006) employ the parameter vector of an Output Error (OE) model and statistical hypothesis testing procedures in order to tackle damage diagnosis in a six-story building model under earthquake excitation. Nair and Kiremidjian (2007) employ Gaussian mixture modelling of the parameter vector of an ARMA model to tackle damage detection on the ASCE benchmark structure. Zheng and Mita (2007) apply a two-stage damage diagnosis method (though not in a statistical context)

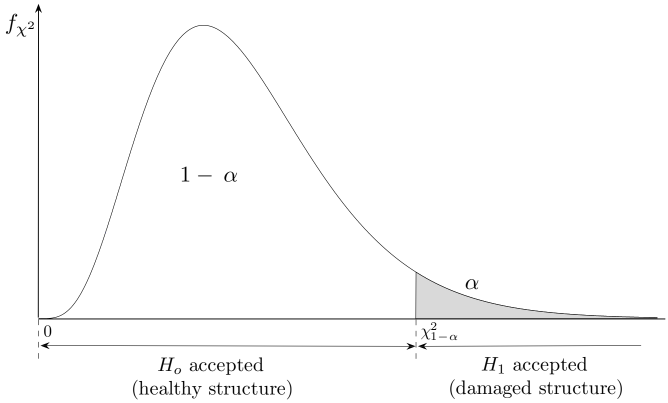

Figure 7. Statistical hypothesis testing based on a χ^2 distributed statistic (one-tail test).

on a five-storey steel structure. Damage detection is achieved in the first stage using the distance between two ARMA models, while damage localization is achieved in the second stage via pre-whitening filters. Carden and Brownjohn (2008) use ARMA model parameters for damage detection and identification in the IASC-ASCE benchmark four-story frame structure, in the Z24 bridge, and in the Malaysia-Singapore Second Link bridge. Hios and Fassois (2009b) employ the model parameter vector, or, alternatively, the modal parameters, of a global Functionally Pooled VAR model for damage detection in a smart composite beam under varying temperature. Mosavi et al. (2012) employ the distances between the parameters of Vector AR (VAR) models in order to detect and localize damage in a two-span continuous steel beam subject to ambient vibrations. In the non-linear model case Wei et al. (2005) use Non-linear AutoRegressive Moving Average with eXogenous excitation (NARMAX) models for fault detection and identification in carbon fiber-reinforced epoxy plates based on a deterministic index, which mirrors changes incurred in the modal parameters.

5.2 Model Residual Based Methods

Model residual based methods tackle damage detection and identification using characteristic quantities that are functions of the residual sequences obtained by driving the current signal(s) Z_u through suitable and predetermined (in the baseline phase) models $\mathcal{M}_o, \mathcal{M}_A, \mathcal{M}_B, \ldots$, each one corresponding to a particular structural state. The general idea is that

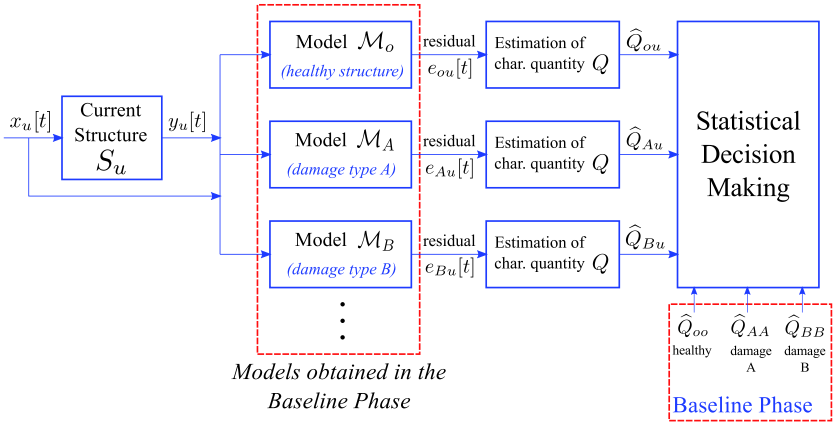

Figure 8. Schematic representation of a "general" residual based statistical time series SHM method (the operations associated with the baseline phase are within the dashed boxes).

the residual sequence obtained by a model that truly reflects the current structural state possesses certain distinct properties, and is thus possible to distinguish. An advantage of the methods is that no model re-identification is required in the inspection phase. The methods have a long history of development and application, mainly within the more general context of engineering systems (Basseville and Nikiforov, 1993; Natke and Cempel, 1997; Gertler, 1998).

Let $\mathcal{M}_V$ designate the model representing the structure in its V state ($V = o$ or $V = A, B, \ldots$). The residual series obtained by driving the current signal(s) Z_u through each one of the aforementioned models are designated as $e_{ou}[t], e_{Au}[t], e_{Bu}[t], \ldots$ and are characterized by variances $\sigma^2_{ou}, \sigma^2_{Au}, \sigma^2_{Bu}, \ldots$, respectively. Notice that the first subscript designates the model employed, while the second the structural state corresponding to the currently used excitation and/or response signal(s). The characteristic quantities obtained from the corresponding residual series are designated as $Q_{ou}, Q_{Au}, Q_{Bu}, \ldots$. On the other hand, the characteristic quantities obtained using the baseline data records are designated as Q_{VV} ($V = o$ or $V = A, B, \ldots$). A schematic representation for a "general" (generic) residual based SHM method is illustrated in Figure 8.

A residual variance based method. In this case the characteristic quantity is the variance of the model residual sequence. Damage detection is based on the fact that the residual series $e_{ou}[t]$, obtained by driving the current signals Z_u through the model $\mathcal{M}_o$ corresponding to the nominal (healthy) structure, should be characterized by variance $\sigma_{ou}^2 = \sigma_{oo}^2$ which becomes minimal if and only if the current structure is healthy ($S_u = S_o$).

Damage detection is thus based on the following hypothesis testing problem:

$$\begin{array}{ll} H_o: & \sigma_{ou}^2 \leq \sigma_{oo}^2 \text{ (null hypothesis – healthy structure)} \\ H_1: & \sigma_{ou}^2 > \sigma_{oo}^2 \text{ (alternative hypothesis – damaged structure).} \end{array} \tag{30}$$

Under the null (H_o) hypothesis, the residuals $e_{ou}[t]$ are (just like the residuals $e_{oo}[t]$) iid Gaussian with zero mean and variance σ_{oo}^2. Hence the quantities $N_u\widehat{\sigma}_{ou}^2/\sigma_{oo}^2$ and $(N_o - d)\widehat{\sigma}_{oo}^2/\sigma_{oo}^2$ follow central χ^2 distributions with N_u and $N_o - d$ degrees of freedom, respectively (as sums of squares of independent standardized Gaussian random variables; see Appendix). Note that N_o and N_u designate the number of samples used in estimating the residual variance in the healthy and current cases, respectively (typically $N_o = N_u = N$), and d designates the dimensionality of the estimated model parameter vector. N_u and N_o should be adjusted to $N_u - 1$ and $N_o - 1$, respectively, in case each estimated mean is subtracted from each residual sequence. Consequently, the following statistic follows $\mathcal{F}$ distribution with $(N_u, N_o - d)$ degrees of freedom (as the ratio of two independent and normalized χ^2 random variables; see Appendix):

$$\text{Under } H_o: \quad F = \frac{\frac{N_u\widehat{\sigma}_{ou}^2}{\sigma_{oo}^2 N_u}}{\frac{(N_o-d)\widehat{\sigma}_{oo}^2}{\sigma_{oo}^2(N_o-d)}} = \frac{\widehat{\sigma}_{ou}^2}{\widehat{\sigma}_{oo}^2} \sim \mathcal{F}(N_u, N_o - d). \tag{31}$$

The following test is thus constructed at the α (false alarm) risk level (Figure 9):

$$\begin{array}{lll} F \leq f_{1-\alpha}(N_u, N_o - d) & \Longrightarrow H_o \text{ is accepted} & \text{(healthy structure)} \\ \text{Else} & \Longrightarrow H_1 \text{ is accepted} & \text{(damaged structure)} \end{array} \tag{32}$$

with $f_{1-\alpha}(N_u, N_o - d)$ designating the corresponding $\mathcal{F}$ distribution's $1-\alpha$ critical point.

Damage identification may be similarly achieved via pairwise tests of the form:

$$\begin{array}{ll} H_o: & \sigma_{Xu}^2 \leq \sigma_{XX}^2 \text{ (structure under damage type } X) \\ H_1: & \sigma_{Xu}^2 > \sigma_{XX}^2 \text{ (structure not under damage type } X). \end{array} \tag{33}$$

An alternative possibility could be based on obtaining the residual series $e_{Au}[t]$, $e_{Bu}[t]$, ... Then, the current damage type is determined as that

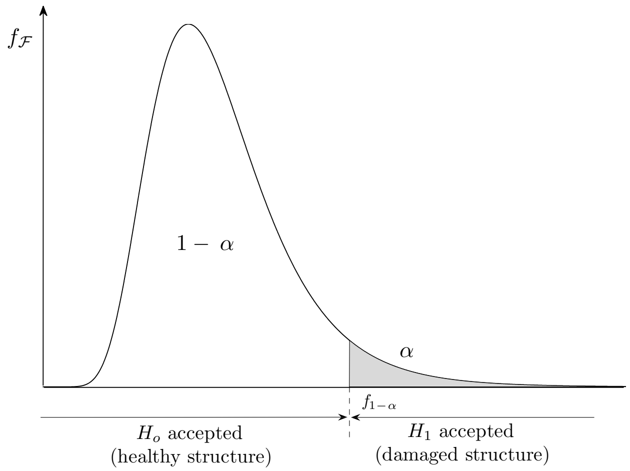

Figure 9. Statistical hypothesis testing based on an $\mathcal{F}$ distributed statistic (one-tail test).

one for which the residual series is characterized by minimal variance – notice that by including the residual sequence $e_{ou}[t]$ in the test, both damage detection and identification may be achieved. On the other hand, damage quantification may be possibly achieved in the limited case of a single damage type by associating specific values of the residual variance with specific damage magnitudes.

Bibliographical remarks. Sohn et al. (2001) use the prediction errors of a so-called AutoRegressive and AutoRegressive with eXogenous inputs (AR-ARX) model. The method is assessed via numerical simulations and its application to an eight degree-of-freedom mass-spring system, data obtained from a patrol boat, and a three-storey building model. In a related work, Sohn and Farrar (2001) employ the standard deviation ratio of the residuals of a AR-ARX model as the damage sensitive feature to infer the structural health state of an eight degree-of-freedom mass-spring system.

Fugate et al. (2001) use the AR model residuals, along with statistical process control methods, to monitor their mean and variance in order to detect damage on a concrete bridge column. Basseville et al. (2004) present a method based on subspace identification and state space model residuals in order to treat damage detection and localization. Yan et al. (2004) use an

X-bar control chart on state space model residuals for damage detection and identification in an aircraft skeleton and the Z24 bridge benchmark. Lu and Gao (2005) use an ARX model and the standard deviation of its residuals to treat damage detection and localization in a two and eight degree-of-freedom simulated mass-spring system. Sohn et al. (2005) explore the use of extreme value statistics on model residuals in order to classify damage.

An estimate of the standard deviation along with higher-order moments of the residuals obtained from vector AR models are used to detect damage by Mattson and Pandit (2006). A damage detection threshold level is identified from available training data, while the method is assessed via data obtained from an eight degree-of-freedom test bed. Zhang (2007) explores data normalization procedures and a probability based measure expressing changes in the ARX residual variance for damage detection and identification in a three-span continuous girder bridge simulation model. Gao and Lu (2009) present a formulation that enables the construction of residual generators via state-space representations. Damage detection is demonstrated via numerical results and experimental examples on a laboratory test frame. Rao and Ratnam (2012) employ the AR model residuals along with Shewhart and weighted moving average control charts for damage detection and identification in welded structures.

In the time-varying (non-stationary) case Poulimenos and Fassois (2004) employ a Time-varying AutoRegressive with eXogenous excitation (TARX) model along with statistical hypothesis testing employing its residual variance in order to detect faults in a bridge-like structure with moving mass. Spiridonakos and Fassois (2009) tackle fault detection in a time-varying extendable prismatic link structure via Functional Series Vector Time Dependent AutoRegressive (FS-VTAR) model residuals.

Methods employing Neural Network (NN) type non-linear models and deterministic decision making based on the response error (residual) are presented in Masri et al. (2000) and Huang et al. (2003).

A likelihood based method. In this case damage detection is based on the likelihood function under the null hypothesis H_o of a healthy structure (Gertler, 1998, pp. 119–120). The hypothesis testing problem thus is:

$$\begin{aligned} H_o: &\quad \boldsymbol{\theta}_o = \boldsymbol{\theta}_u \text{ (null hypothesis – healthy structure)} \\ H_1: &\quad \boldsymbol{\theta}_o \neq \boldsymbol{\theta}_u \text{ (alternative hypothesis – damaged structure),} \end{aligned} \tag{34}$$

with $\boldsymbol{\theta}_o, \boldsymbol{\theta}_u$ designating the parameter vectors corresponding to the healthy and current structure, respectively. Assuming serial independence of the residual sequence, the Gaussian likelihood function $L_y(Y, \boldsymbol{\theta}/X)$ for the data

Y given X is obtained as (Box et al., 1994, p. 226):

$$L_y(Y, \boldsymbol{\theta}/X) = \frac{1}{\left(\sqrt{2\pi\sigma^2}\right)^N} \cdot \exp\left\{ -\frac{1}{2\sigma^2} \sum_{t=1}^{N} e^2[t, \boldsymbol{\theta}] \right\} \tag{35}$$

with $e[t, \boldsymbol{\theta}]$ designating the model residual (one-step-ahead prediction error) characterized by zero mean and variance σ^2.

Under the null (H_o) hypothesis, the residual series $e_{ou}[t]$ generated by driving the current signal(s) through the nominal model is (just like $e_{oo}[t]$) iid Gaussian with zero mean and variance σ_{oo}^2. Damage detection is then based on the likelihood function under H_o evaluated for the current data, by requiring it to be larger or equal to a (properly selected) threshold l in order for the null (H_o) hypothesis to be accepted:

$$\begin{array}{lcll} L_y(Y, \boldsymbol{\theta}_o/X) \geq l & \Longrightarrow & H_o \text{ is accepted} & \text{(healthy structure)} \\ \text{Else} & \Longrightarrow & H_1 \text{ is accepted} & \text{(damaged structure).} \end{array} \tag{36}$$

Obviously, the evaluation of $L_y(Y, \boldsymbol{\theta}_o/X)$ requires knowledge of the true innovations variance σ_{oo}^2. This is typically a-priori unknown, but it may be estimated quite accurately for long data records ("large" N), in which case its variability may be also neglected. Then, under the null (H_o) hypothesis the statistic $N\widehat{\sigma}_{ou}^2/\widehat{\sigma}_{oo}^2$ follows χ^2 distribution with N degrees of freedom (as the sum of squares of mutually independent standardized Gaussian variables; see Appendix). This leads to the re-expression of the previous decision making rule as:

$$\begin{array}{ll} \chi_N^2 = \frac{N\widehat{\sigma}_{ou}^2}{\widehat{\sigma}_{oo}^2} \leq \chi_{1-\alpha}^2(N) & \Longrightarrow H_o \text{ is accepted (healthy structure)} \\ \text{Else} & \Longrightarrow H_1 \text{ is accepted (damaged structure),} \end{array} \tag{37}$$

with $\chi_{1-\alpha}^2(N)$ designating the χ^2 distribution's $1-\alpha$ critical point. Note that N should be adjusted to $N-1$ in case the estimated mean is subtracted from the residual series $e_{ou}[t]$.

Damage identification may be achieved by computing the likelihood function for the current signal(s) for the various values of $\boldsymbol{\theta}$ ($\boldsymbol{\theta}_A, \boldsymbol{\theta}_B, \ldots$) and accepting the hypothesis that corresponds to the maximum value of the likelihood:

$$\max_V L_y(Y, \boldsymbol{\theta}_V/X) \Longrightarrow H_V \text{ is accepted (damage type } V\text{).} \tag{38}$$

It should be mentioned that damage detection may be also achieved by including $\boldsymbol{\theta}_o$ in the hypothesis testing procedure. Damage quantification may be possibly achieved in the limited case of a single type of damage, by associating specific values of the likelihood with specific damage magnitudes.

A residual uncorrelatedness based method. This method is based on the fact that the residual sequence $e_{ou}[t]$ obtained by driving the current signal(s) Z_u through the nominal model $\mathcal{M}_o$ (resp. $\mathcal{M}_V$) is *uncorrelated* (white) if and only if the current structure is in its nominal (healthy) S_o (resp. S_V). Damage detection may be then based on the following hypothesis testing problem:

$$\begin{array}{ll} H_o: \quad \rho[\tau]=0 \quad \tau=1,2,\ldots,r \\ \text{(null hypothesis – healthy structure)} \\ H_1: \quad \rho[\tau]\neq 0 \quad \text{for some } \tau \\ \text{(alternative hypothesis – damaged structure)} \end{array} \tag{39}$$

with $\rho[\tau]$ being the normalized autocovariance (ACF) function (see Table 7) of the $e_{ou}[t]$ residual sequence. Thus, the method's characteristic quantity is $Q=\big[\rho[1]\ \rho[2]\ \ldots\ \rho[\tau]\big]^T$, with r being a design variable.

Under the null (H_o) hypothesis, the residual sequence $e_{ou}[t]$ is iid Gaussian with zero mean, and the statistic χ^2_ρ, below, follows χ^2 distribution with r degrees of freedom (Box et al., 1994, p. 314):

$$\text{Under } H_o: \quad \chi^2_\rho = N(N+2)\cdot\sum_{\tau=1}^{r}(N-\tau)^{-1}\cdot\widehat{\rho}^2[\tau] \ \sim\ \chi^2(r) \tag{40}$$

with $\widehat{\rho}[\tau]$ designating the estimator of $\rho[\tau]$.

Decision making is then based on the following test at the α (false alarm) risk level:

$$\begin{array}{ccll} \chi^2_\rho \leq \chi^2_{1-\alpha}(r) & \Longrightarrow & H_o \text{ is accepted} & \text{(healthy structure)} \\ \text{Else} & \Longrightarrow & H_1 \text{ is accepted} & \text{(damaged structure)} \end{array} \tag{41}$$

with $\chi^2_{1-\alpha}(r)$ designating the χ^2 distribution's $1-\alpha$ critical point.

Damage identification may be achieved by similarly examining which one of the $e_{Vu}[t]$ (for $V=A,B,\ldots$) residual series is uncorrelated. As with the previous methods, only damages of specific magnitudes (but not the continuum of damage magnitudes) may be considered.

A Sequential Probability Ratio Test (SPRT) based method. This method employs the Sequential Probability Ratio Test (SPRT – Wald 1947; Ghosh and Sen 1991) in order to detect a change in the standard deviation σ_{ou} of the model residual sequence $e_{ou}[t]$. The SPRT based method employs both α (false alarm) and β (missed damage) error probabilities in its design. Damage detection is based on the SPRT of strength (α,β) for the following hypothesis testing problem:

$$\begin{array}{ll} H_o: & \sigma_{ou}\leq\sigma_o \text{ (null hypothesis – healthy structure)} \\ H_1: & \sigma_{ou}\geq\sigma_1 \text{ (alternative hypothesis – damaged structure),} \end{array} \tag{42}$$

with σ_{ou} designating the standard deviation of the residual signal $e_{ou}[t]$ obtained by driving the current signal(s) through the healthy structural model, and σ_o, σ_1 user defined values. The basis of the SPRT is the logarithm of the likelihood ratio function based on n ($n \leq N$) samples:

$$\mathcal{L}(n) = \sum_{t=1}^{n} \ln \frac{f(e_{ou}[t]|H_1)}{f(e_{ou}[t]|H_o)} = n \cdot \ln \frac{\sigma_o}{\sigma_1} + \frac{\sigma_1^2 - \sigma_o^2}{2\sigma_o^2\sigma_1^2} \cdot \sum_{t=1}^{n} e_{ou}^2[t] \tag{43}$$

with $f(e_{ou}[t]|H_i)$ designating the probability density function of the residual sequence under hypothesis H_i ($i = 0, 1$).

Decision making is then based on the following test at the (α, β) risk levels:

$$\begin{array}{rcll} \mathcal{L}(n) \leq B & \Longrightarrow & H_o \text{ is accepted} & \text{(healthy structure)} \\ \mathcal{L}(n) \geq A & \Longrightarrow & H_1 \text{ is accepted} & \text{(damaged structure)} \\ B < \mathcal{L}(n) < A & \Longrightarrow & \text{no decision is made} & \text{(continue the test)} \end{array} \tag{44}$$

with:

$$A = \ln \frac{1-\beta}{\alpha} \quad \text{and} \quad B = \ln \frac{\beta}{1-\alpha}. \tag{45}$$

Following a decision at a stopping time $\widehat{n}$, it is possible to continue the test by resetting $\mathcal{L}(\widehat{n}+1)$ to zero and using additional residual samples.

Damage identification may be achieved by performing SPRTs similar to the above separately for damages of each potential type.

Bibliographical remarks. Sohn et al. (2003a) combine the SPRT with extreme value statistics for treating statistical damage classification in a laboratory three-story building model, while Oh and Sohn (2009) use the SPRT to tackle damage diagnosis under environmental and operational variations. Kopsaftopoulos and Fassois (2011) use the SPRT in order to detect and identify damage in a scale aircraft skeleton structure.

5.3 Functional Model (FM) Based SHM Methods

The Functional Model (FM) based methods provide a *unified framework* for the combined treatment of the damage detection, identification (localization), and quantification (magnitude estimation) subproblems. An important asset of the methods is overcoming the limitation of treating damages occurring *only* at *specific and pre-specified* locations and of *specific magnitudes*. Indeed, FM methods allow for the full and complete treatment of damages, achieving precise *localization* over *continuous topologies* on a structure and over the *continuum* of all damage magnitudes.

The cornerstone of the methods is the new class of *Functional Models (FMs)*, which allows for the analytical inclusion of *both* damage location and magnitude information (Kopsaftopoulos and Fassois, 2006; Sakellariou and Fassois, 2007; Hios and Fassois, 2009a,c). FM models essentially permit the extension of the notion of *damage mode* to include damage not only of all possible magnitudes, but also of all possible *locations* on a specific (continuous) topology on a structure. FMs are based on the *pooling* of multiple data records, thus they are also referred to as *Functionally Pooled* (FP) models, and are explicitly parametrized in terms of both damage location and magnitude. In the simple, special, case where only a finite number (instead of a continuum) of damage locations is considered, the parametrization may be limited to damage magnitude alone (Sakellariou and Fassois, 2008). This case is treated in the sequel for the sake of simplicity and clarity. Information on the more general case is provided in the bibliographical remarks.

Let the damage magnitude, within a specific damage mode (type) V, be represented by a scalar variable $k \in \mathbb{R}$. The healthy structure typically corresponds to $k = 0$. Then, a simple model capable of representing the structural dynamics under mode V is the *Functionally Pooled AutoRegressive with eXogenous excitation (FP-ARX)* model:

$$y_k[t] + \sum_{i=1}^{na} a_i(k) \cdot y_k[t-i] = \sum_{i=0}^{nb} b_i(k) \cdot x_k[t-i] + w_k[t] \tag{46a}$$

$$w_k[t] \sim \text{iid}\, \mathcal{N}\big(0, \sigma_w^2(k)\big), \quad k \in \mathbb{R} \tag{46b}$$

$$a_i(k) = \sum_{j=1}^{p} a_{i,j} \cdot G_j(k), \quad b_i(k) = \sum_{j=1}^{p} b_{i,j} \cdot G_j(k). \tag{46c}$$

In this expression $x_k[t]$, $y_k[t]$, and $w_k[t]$ designate the excitation, response, and innovations (residual) signals, respectively, corresponding to a specific damage magnitude k. The form of the model resembles that of a conventional ARX. Yet, its AR and X parameters, as well as its innovations variance, are explicit functions of the damage magnitude k, belonging to p-dimensional functional subspaces spanned by the mutually independent basis functions $G_1(k)$, $G_2(k)$, ..., $G_p(k)$ (*functional basis*). The constants $a_{i,j}$ and $b_{i,j}$ designate the AR and X, respectively, coefficients of projection. The parameter vector to be estimated from the measured signals is $\boldsymbol{\theta} = [\alpha_{i,j} \vdots b_{i,j}]^T$.

In the *baseline phase*, a suitable FP model, corresponding to each considered damage mode, is estimated using signals obtained under various damage magnitudes k. In the *inspection phase*, given the current signal(s)

Z_u, damage detection is based on the FP-ARX model of damage mode V (or in fact any other). This is now re-parametrized in terms of the currently unknown damage magnitude k and the innovations variance $\sigma^2_{e_u}$ ($e_u[t]$ designates the re-parametrized model's innovations), by replacing the coefficients of projection by their corresponding estimates available from the baseline phase:

$$\mathcal{M}_V(k, \sigma^2_{e_u}) : \ y_u[t] + \sum_{i=1}^{na} a_i(k) \cdot y_u[t-i] = \sum_{i=0}^{nb} b_i(k) \cdot x_u[t-i] + e_u[t]. \quad (47)$$

Damage detection is based on the following hypothesis testing problem:

$$\begin{array}{lll} H_o: & k = 0 & \text{(null hypothesis – healthy structure)} \\ H_1: & k \neq 0 & \text{(alternative hypothesis – damaged structure).} \end{array} \quad (48)$$

Estimates of k and $\sigma^2_{e_u}$ are obtained based on the current data Z_u and the Nonlinear Least Squares (NLLS) estimator (refer to Ljung 1999, pp. 327–329 for details on NLLS estimation):

$$\widehat{k} = \arg\min_k \sum_{t=1}^{N} e_u^2[t], \qquad \widehat{\sigma}^2_{e_u} = \frac{1}{N} \sum_{t=1}^{N} \widehat{e}_u^2[t]. \quad (49)$$

Assuming that the structure is indeed under a damage belonging to mode V (or in healthy condition which simply corresponds to $k = 0$), the above estimator may be shown to be asymptotically ($N \to \infty$) Gaussian, with mean equal to its true value k and variance σ^2_k provided by the Cramer-Rao lower bound (Sakellariou and Fassois, 2008):

$$\widehat{k} \sim \mathcal{N}(k, \sigma^2_k). \quad (50)$$

Under the null hypothesis H_o, the t statistic, below, follows t distribution with $N-1$ degrees of freedom (to be adjusted to $N-2$ in case the estimated mean is subtracted from the residuals in the evaluation of $\widehat{\sigma}_k$; see Appendix):

$$t = \widehat{k}/\widehat{\sigma}_k \ \sim \ t(N-1) \quad (51)$$

which leads to the following test at the α (false alarm) risk level:

$$\begin{array}{ll} t_{\frac{\alpha}{2}}(N-1) \leq t \leq t_{1-\frac{\alpha}{2}}(N-1) \Longrightarrow & H_o \text{ is accepted (healthy structure)} \\ \text{Else} \qquad \Longrightarrow & H_1 \text{ is accepted (damaged structure)} \end{array} \quad (52)$$

with t_α designating the t distribution's α critical point.

Once damage is detected, *damage mode identification* is achieved through successive estimation and validation of the re-parametrized model $\mathcal{M}_V(k, \sigma_{e_u}^2)$ of Equation (47) of each damage mode ($V = A, B, \ldots$) using the current signal(s) Z_u. The procedure terminates as soon as a particular model is successfully validated, with the corresponding damage mode identified as current. Model validation may be based on statistical tests examining the hypothesis of residual uncorrelatedness (see section 5.2).

Following this, an *interval estimate* (at the α risk level) of the damage magnitude k is then obtained based on the point estimates $\widehat{k}$ and $\widehat{\sigma}_k$:

$$k \text{ interval estimate:} \quad \left[\widehat{k} + t_{\frac{\alpha}{2}}(N-1)\cdot\widehat{\sigma}_k,\ \widehat{k} + t_{1-\frac{\alpha}{2}}(N-1)\cdot\widehat{\sigma}_k\right]. \quad (53)$$

Bibliographical remarks. Sakellariou et al. (2002) and Sakellariou and Fassois (2008) present the application of an FM based method which considers a finite number of fault locations for on-board fault detection in railway vehicle systems, and damage detection, localization and magnitude estimation in a scale aircraft skeleton structure, respectively. Kopsaftopoulos and Fassois (2007, 2012) postulate the generalization of the FM based method in order to include damage not only of all possible magnitudes, but also of all possible locations on continuous topologies on a structure. The method's effectiveness is assessed via its application to damage detection, precise localization and magnitude estimation on a scale aircraft skeleton structure.

6 Application of the Methods to a Laboratory Truss Structure

6.1 The Laboratory Truss Structure and Problem Definition

The use of various methods is now illustrated through their application to damage diagnosis on a laboratory truss structure. The structure and part of the experimental set-up are shown in Figure 10. It consists of twenty eight elements with rectangular cross sections (15×15 mm) jointed together via steel elbow plates and bolts. All parts are constructed from standard aluminium with the overall dimensions being $1400 \times 700 \times 800 \times 700$ mm.

The damages considered correspond to complete loosening of various bolts at different joints of the structure. Five distinct types, each corresponding to the loosening of bolts joining together various horizontal, vertical and diagonal elements, are considered (Table 8 and Figure 10).

The structure is suspended through a set of cords and is excited vertically at Point X through an electromechanical shaker (MB Dynamics Modal 50A, max load 225 N) equipped with a stinger (Figure 10). The force excitation is

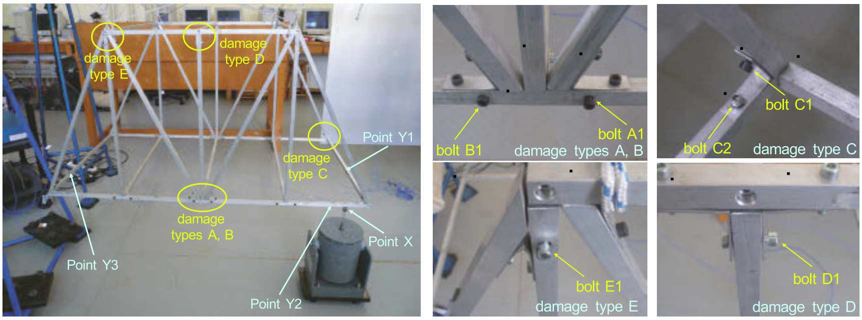

Figure 10. The aluminum truss structure and the experimental set-up: The force excitation (Point X), the vibration measurement positions (Points Y1, Y2, Y3), and the considered damage types (A, B, C, D, and E).

Table 8. The considered damage types and experimental details.

Structural State	Description	No of Experiments
Healthy	—	40 (1 baseline)
Damage type A	loosening of bolt A1	32 (1 baseline)
Damage type B	loosening of bolts A1 and B1	32 (1 baseline)
Damage type C	loosening of bolts C1 and C2	32 (1 baseline)
Damage type D	loosening of bolt D1	32 (1 baseline)
Damage type E	loosening of bolt E1	32 (1 baseline)

Sampling frequency: $f_s = 256$ Hz, Signal bandwidth: $[0.5 - 100]$ Hz
Signal length N in samples (s): Non-parametric methods: $N = 30\ 720$ (120 s)
Parametric methods: $N = 10\ 000$ (39 s)

a random Gaussian signal measured via an impedance head (PCB 288D01, sensitivity 98.41 mV/lb), while the resulting strain responses are measured at different points via dynamic strain gauges (PCB ICP 740B02, $0.005-100$ kHz, 50 mV/$\mu\varepsilon$). The analysis bandwidth is $0.5 - 100$ Hz and the sampling frequency $f_s = 256$ Hz. The measured signals are driven through a signal conditioning device (PCB 481A02) into the data acquisition system (SigLab 20–42). In this study damage detection and identification is based on one of the three vibration response signals (Points Y1, Y2 and Y3 – Figure 10) at a time, so that *scalar* (univariate) versions of the methods are used.

Experimental details and the number of experiments for each damage type are presented in Table 8. One experiment per damage type is executed in the baseline phase, while several are executed in the inspection phase. The excitation and response signals are in all cases pre-processed, so that the sample mean is subtracted and each signal is normalized by its sample standard deviation.

Both response-only and excitation-response methods are used. In all cases, the fact that only a single response is used and also in a very limited bandwidth, renders the damage diagnosis problem challenging. This allows for the exploration of the capabilities and limitations of the methods when very limited information is available.

6.2 Baseline Phase: Structural Identification

Non-parametric identification. Non-parametric identification is based on $N = 30\ 720$ (≈ 120 s) sample-long excitation and/or response signals.

Sample response PSD and FRF magnitude estimates for the healthy and various damage states of the structure are depicted in Figure 11 for response Y3 (MATLAB functions *pwelch.m* and *tfestimate.m*, respectively – details in Table 9). It is evident that the healthy and damage estimates are quite similar in the $0.5 - 30$ Hz range, where the first twelve modes are included. Significant discrepancies between the healthy and damage type C, D and E curves are observed in the $30 - 58$ Hz range, where the next three modes are included. These discrepancies become even more evident for damage types C and E in the $58 - 100$ Hz range, where the next eight modes are included. Figure 12 depicts the Welch based FRF magnitude estimates for the healthy and damage type A structural states, along with their corresponding 95% confidence intervals (refer to Table 7). Although both FRF magnitude curves are quite similar, small discrepancies are evident at specific frequencies. Yet the statistical significance of these discrepancies has to be confirmed.

Parametric identification. In the parametric case only excitation-response representations are presently employed. Estimation is based on $N = 10\ 000$ (≈ 39 s) sample-long excitation and response signals which are used for estimating AutoRegressive with eXogenous excitation (ARX) models (MAT-

Table 9. Non-parametric estimation details.

Data length	$N = 30\ 720$ samples (≈ 120 s)
Method	Welch, zero overlap
Segment length (samples)	$L = 2\ 048$ samples
No of non-overlapping segments	$K = 15$ segments
Window type	Hamming
Frequency resolution	$\Delta f = 0.125$ Hz

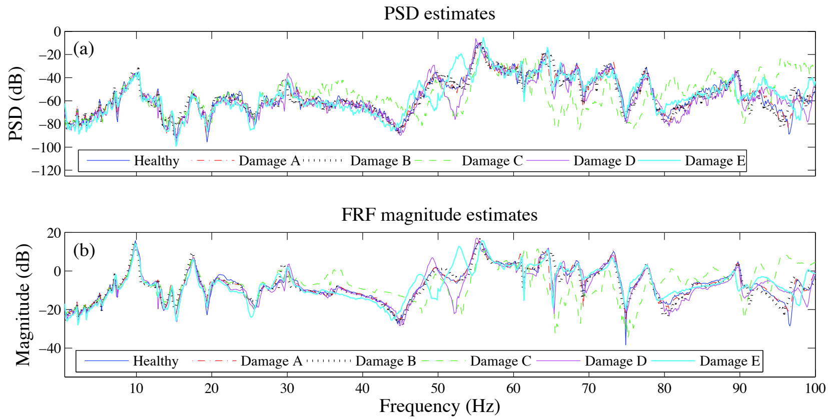

Figure 11. Indicative non-parametric (Welch based) estimates for the healthy and damaged structural states (response Y3): (a) Power Spectral Density (PSD) and (b) Frequency Response Function (FRF) magnitude estimates.

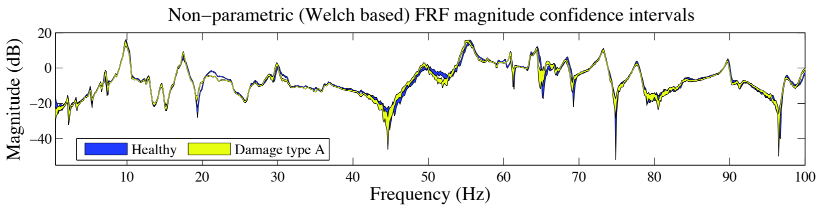

Figure 12. Non-Parametric (Welch based) FRF magnitude estimates for the healthy and damage type A structural states along with their 95% confidence intervals (response Y3).

LAB function *arx.m*). The modelling strategy consists of the successive fitting of ARX(na, nb) models ($na = nb = n$ is presently used) until a suitable model is selected. Model parameter estimation is based on minimization of a quadratic Prediction Error (PE) criterion leading to a Least Squares (LS) estimator (Ljung 1999, p. 206, Fassois 2001). Model order selection, which is crucial for successful identification, is based on a combination of tools, including the Bayesian Information Criterion (BIC – Figure 13a), the RSS/SSS (Residual Sum of Squares over Signal Sum of Squares – Figure 13b), residual series whiteness, and "stabilization diagrams".

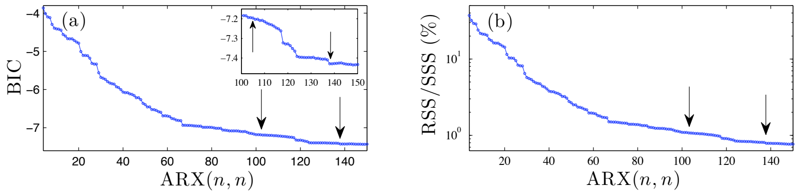

Figure 13. Order selection criteria for ARX(n,n) type parametric models in the healthy case (response Y3): (a) BIC and (b) RSS/SSS.

Table 10. Selected models and estimation details.

Response	Selected Model	No parameters	SPP	BIC	RSS/SSS (%)
Y1	ARX(112, 112)	225 parameters	44.4	−5.19	0.43
Y2	ARX(136, 136)	273 parameters	36.6	−5.83	0.22
Y3	ARX(103, 103)	207 parameters	48.3	−4.31	1.07
Parameter estimation method: Weighted Least Squares (WLS)					
Signal length: $N = 10\ 000$ samples (≈ 39 s)					

The identification procedure leads to the selection of an ARX(112, 112), an ARX(136, 136) and an ARX(103, 103) model for vibration responses Y1, Y2 and Y3, respectively. The selected ARX models, as well as their estimation details, numbers of estimated parameters, signal Samples Per Parameter (SPP), BIC, and RSS/SSS values are summarized in Table 10. Figure 14 presents a comparison between the parametric (response Y3 – ARX(103, 103) based) FRF magnitude estimate and its non-parametric (Welch based) counterpart; the agreement is excellent.

6.3 Inspection Phase: SHM via Selected Non-Parametric Methods

PSD based method. Typical PSD based damage detection results are presented in Figure 15 based on response Y3. Evidently, correct detection at the $\alpha = 10^{-4}$ risk level is achieved in each case, as the test statistic is shown not to exceed the critical points (dashed horizontal lines) in the healthy case, while it exceeds them in each damage case. In each case the sensor location with respect to the damage location is characterized as "local" or "remote". Observe that damage type C (two bolts loosened) is the easiest to detect (note the logarithmic scale on the vertical axis of Figure 15), while damage type A (one bolt loosened) is the hardest (the test statistic is within the

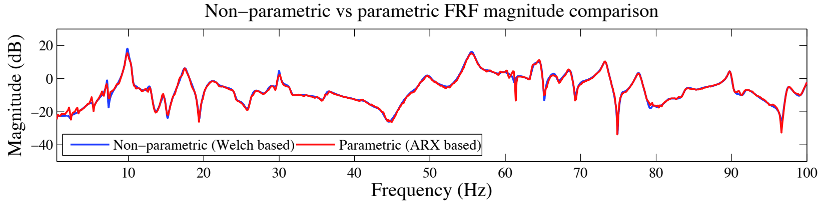

Figure 14. Parametric (ARX based) and non-parametric (Welch based) FRF magnitude estimates for the healthy structure (response Y3).

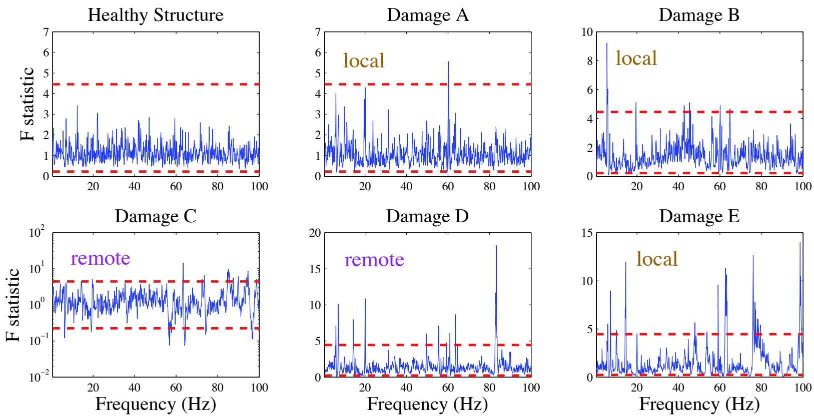

Figure 15. PSD based damage detection (response Y3): Indicative results at the $\alpha = 10^{-4}$ risk level. "Local" and "remote" damages are considered with the actual structural state indicated above each plot box. A damage is detected if the test statistic exceeds the critical points (dashed horizontal lines).

critical points for most frequencies).

Representative damage identification results are, at the $\alpha = 10^{-4}$ risk level, presented in Figure 16 based on response Y1. The actual damage is of type A. When testing the hypothesis of damage type A, the test statistic does not exceed the critical points, while it clearly exceeds them when testing any other hypothesis.

FRF based method. Figure 17 presents typical FRF based damage detection results based on response Y2. In each case the sensor location with

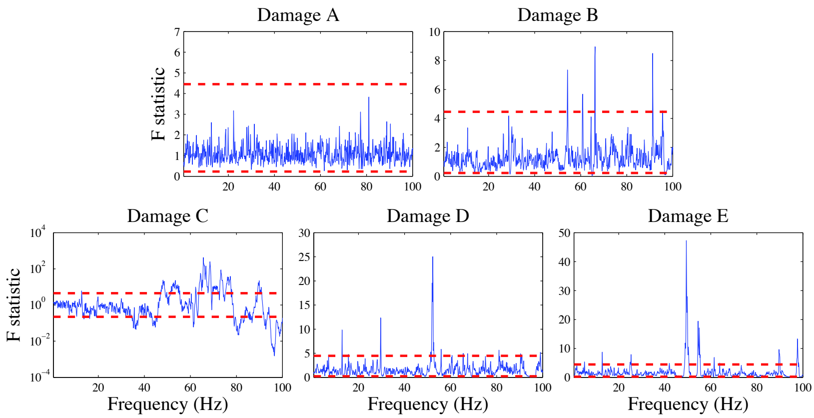

Figure 16. PSD based damage identification (response Y1): Indicative results at the $\alpha = 10^{-4}$ risk level, with the actual damage being of type A ("remote" to the sensor location). Each considered hypothesis is shown above each plot box. A hypothesis is accepted as true if the corresponding test statistic does not exceed the critical points (dashed horizontal lines).

respect to the damage location is characterized as "local" or "remote". Correct detection at the $\alpha = 10^{-5}$ risk level is achieved in each case, as the test statistic is shown not to exceed the critical points (dashed horizontal lines) in the healthy case, while it exceeds them in each damage case. Like before, damage type C is the easiest to detect, while damage types A and B are the hardest.

Indicative damage identification results at the $\alpha = 10^{-5}$ risk level are presented in Figure 18 based on response Y1. The actual damage is of type C. When testing the damage type C hypothesis the statistic does not exceed the critical points, while it clearly does so when testing any other hypothesis.

6.4 Inspection Phase: SHM via Selected Parametric Methods

Model parameter based method. The model parameter based method (excitation-response case) is based on the ARX models (Table 10) obtained in the baseline phase, as well as on their counterparts obtained in the inspection phase using the current data records Z_u.

Figure 19 presents typical parametric damage detection results based on the excitation–Y2 response pair. Correct detection is achieved at the $\alpha = 10^{-12}$ risk level, as the test statistic does not exceed the critical point

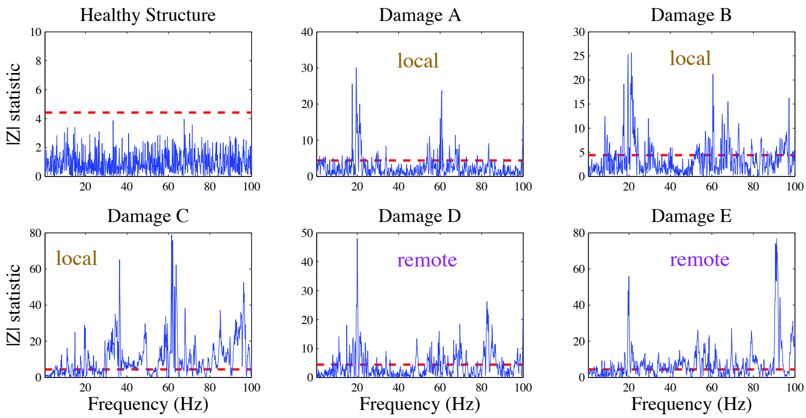

Figure 17. FRF based damage detection (response Y2): Indicative results at the $\alpha = 10^{-5}$ risk level. “Local” and “remote” damages are considered with the actual structural state indicated above each plot box. A damage is detected if the test statistic exceeds the critical point (dashed horizontal line).

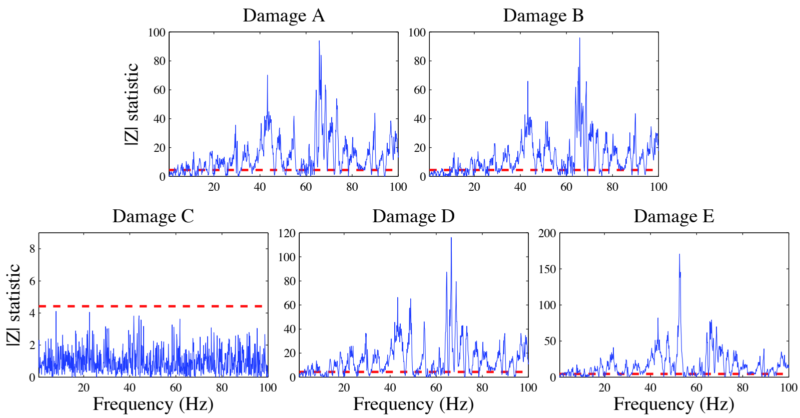

Figure 18. FRF based damage identification (response Y1): Indicative results at the $\alpha = 10^{-5}$ risk level, with the actual damage being of type C (“local” to the sensor location). Each considered hypothesis is shown above each plot box. A hypothesis is accepted as true if the corresponding test statistic does not exceed the critical point (dashed horizontal line).

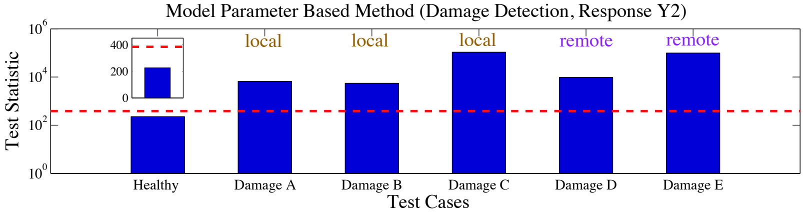

Figure 19. Model parameter based damage detection (excitation–Y2 response): Indicative results at the $\alpha = 10^{-12}$ risk level. "Local" and "remote" damages are considered and characterized above each bar. A damage is detected if the test statistic (bar) exceeds the critical point (dashed horizontal line).

in the healthy case, while it exceeds it in each damage case. Note the logarithmic scale on the vertical axis, indicating significant differences in the statistic between the healthy and the damage cases. The ability of the method to properly identify the damage type is demonstrated in Figure 20 at the $\alpha = 10^{-12}$ risk level using the excitation–Y3 response pair (two test cases are shown).

Residual likelihood based method. This method is based on the ARX models identified in the baseline phase (Table 10). No identification is required in the inspection phase.

Typical damage detection results are presented in Figure 21 based on the excitation–Y1 response pair. Correct detection is achieved at the $\alpha = 10^{-12}$ risk level as the test statistic does not exceed the critical point in the healthy case while exceeding it in each damage case. Damage identification results (two test cases) are presented in Figure 22 based on the excitation–Y3 response pair. In each test case correct identification is achieved at the $\alpha = 10^{-12}$ risk level – it is worth noting the logarithmic scale on the vertical axis.

SPRT based method. Like in the previous method the ARX models identified in the baseline phase (Table 10) are used, with no identification required in the inspection phase.

Typical damage detection results are presented in Figure 23 based on the excitation–Y2 response pair. The characterization of each damage as "local" or "remote" to the response sensor is indicated in each subplot. A

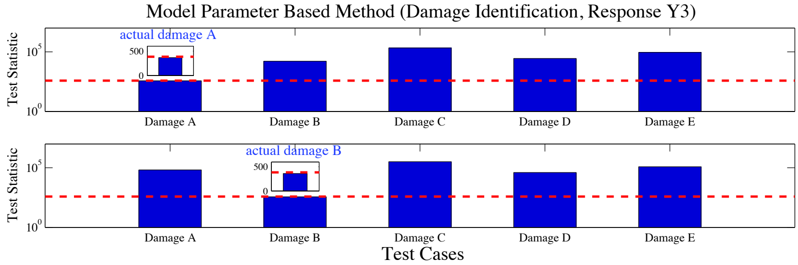

Figure 20. Model parameter based damage identification (excitation–Y3 response): Two indicative test cases at the $\alpha = 10^{-12}$ risk level. The actual damage is indicated in each test case (subplot). A hypothesis is accepted as true if the corresponding test statistic (bar) does not exceed the critical point (dashed horizontal line).

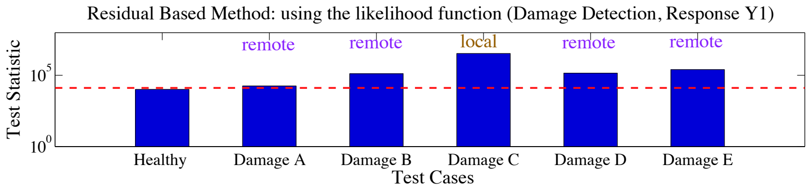

Figure 21. Residual likelihood based damage detection (excitation–Y1 response): Indicative results at the $\alpha = 10^{-12}$ risk level. “Local” and “remote” damages are considered above each bar. A damage is detected if the test statistic (bar) exceeds the critical point (dashed horizontal line).

damage is detected when the test statistic exceeds the *upper* critical point (upper dashed line), while the structure is detected as healthy when the test statistic exceeds the *lower* critical point (lower dashed line). After a critical point is exceeded and a decision is made, the test statistic is reset to zero and the test continues. Evidently, correct detection, at the $\alpha = \beta = 0.01$ risk levels ($q = 1.1$), is obtained in each test case, as the test statistic is shown to exceed multiple times the lower critical point in the healthy case, while it repeatedly exceeds the upper critical point in each damage test case. Observe that damage type A appears harder to detect, as the number of detections in this case is lowest among those of the various damage types, while damage types C and E appear easiest to detect. This is in agreement

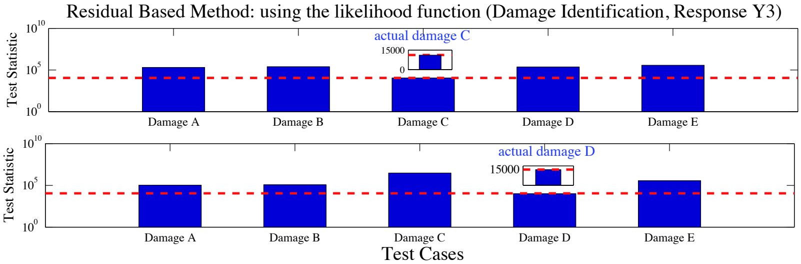

Figure 22. Residual likelihood based damage identification (excitation–Y3 response): Two indicative results at the $\alpha = 10^{-12}$ risk level. The actual damage is indicated in each case (subplot). A hypothesis is accepted as true if the corresponding test statistic (bar) does not exceed the critical point (dashed horizontal line).

with the remarks made in subsection 6.2 and Figure 11.

The ability of the method to identify damage is demonstrated via the test case of Figure 24 based on the excitation–Y3 response pair. The actual damage type (type B) is properly identified as the test statistic exceeds (for the corresponding hypothesis) the lower critical point.

6.5 Discussion

Summary results for all test cases considered and for each one of the three vibration responses (Y1, Y2 and Y3) are presented in Table 11. Evidently, both non-parametric and parametric methods achieve accurate damage detection with mostly zero false alarms at the selected risk levels. Only the FRF based method exhibits one and two false alarms for the vibration responses Y1 and Y3, respectively. The ability of the methods to effectively detect damage is demonstrated by the fact that no missed damage cases are observed. The damage identification results confirm the ability of the methods to accurately identify the damage type. No damage misclassifications are observed, except for the FRF based method where misclassification errors occur for damage type A (Table 11).

It is important to emphasize that these results are achieved using a *single* vibration response signal, or a *single* excitation-response pair, and also a particularly *low frequency range* (0.5 – 100 Hz). It is well known that the problem is more challenging in a “low” frequency range, yet the results demonstrate that it is properly handled without the need for higher frequency ranges. The fact that the methods are capable of detecting and

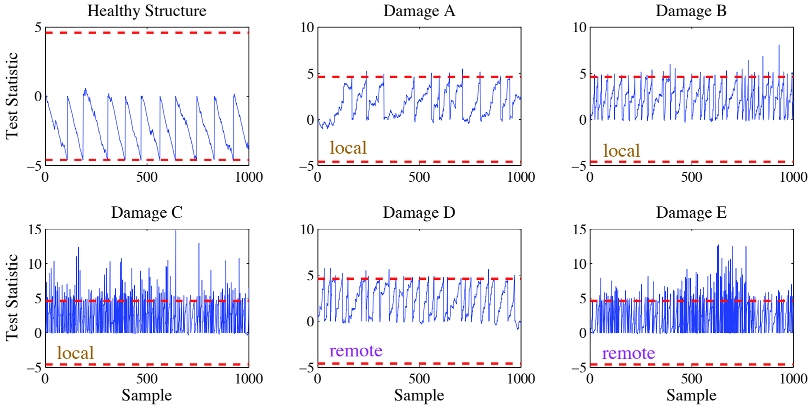

Figure 23. SPRT based damage detection (excitation–Y2 response): Indicative results at the $\alpha = \beta = 0.01$ risk levels ($q = 1.1$). "Local" and "remote" damages are considered with the actual structural state indicated above each plot box. A damage is detected if the test statistic exceeds the *upper* critical point (upper dashed line), while the structure is in its healthy state when the test statistic exceeds the *lower* critical point (lower dashed line).

identifying damage using response sensors that are relatively close ("local") or far ("remote") from the actual damage location should be also emphasized. Of course, performance is somewhat affected by distance; this is demonstrated for the damage type A case in conjunction with the FRF magnitude based method where the lowest misclassification rate occurs for sensor Y2 (Table 11) which is closest to the damage location. Yet, the ability of the methods in this respect is remarkable and underscores the fact that a few (or even a single) vibration response sensors may be adequate for proper detection and identification.

Nevertheless, in using statistical time series SHM methods, a number of issues require attention on part of the user. First, careful model identification, especially in the parametric case, is crucial for successful damage diagnosis. Parametric models require accurate parameter estimation and model structure selection in order to properly represent the structural dynamics and be effectively used for damage diagnosis. Therefore parametric methods require adequate user expertise and are somewhat more elaborate than their non-parametric counterparts.

Another issue of primary importance is the proper selection of the α

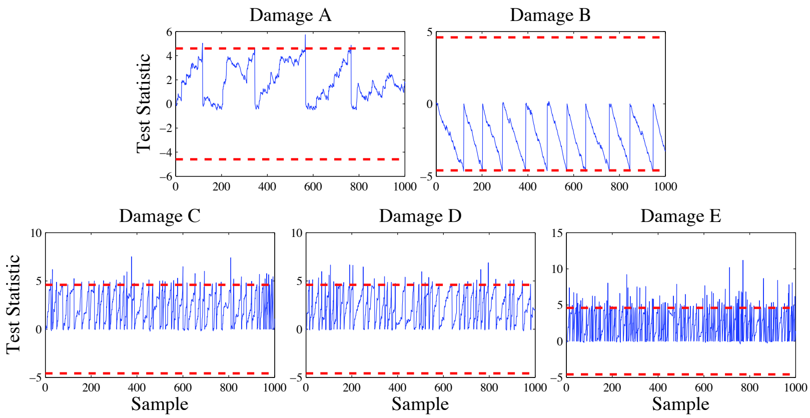

Figure 24. SPRT based damage identification (excitation–Y3 response): Indicative results at the $\alpha = \beta = 0.01$ risk levels ($q = 1.1$), with the actual damage being of type B ("local" to the sensor location). Each considered hypothesis is indicated above each plot box. A hypothesis is accepted as true if the corresponding test statistic exceeds the *lower* critical point (lower dashed line).

(false alarm) risk level. If not properly adjusted, false alarm, missed damage, and damage misclassification cases may occur. The user is advised to make an initial investigation on false alarm rates for different α levels using several healthy data sets. Afterwards, potential missed damage cases may be checked with data corresponding to various damaged structural states. When applying the model residual uncorrelatedness based method, the user should be aware of the fact that the selected max lag r value may affect performance. Thus, a tentative inquiry on this affects the false alarm rate should be undertaken.

Moreover, in order for most parametric methods to work effectively, a very small value of α is very often required. This is due to the fact that the current time series models are incapable of fully capturing the experimental, operational and environmental uncertainties based on just a *single* data record (Hios and Fassois, 2009a; Michaelides and Fassois, 2008). For this reason, a very small α is often selected in order to compensate for the lack of proper uncertainty modelling. This is the subject of on-going research efforts.

It should be noted that only detection is possible for damage types not modeled in the baseline phase, while essentially no work is reported on mul-

Table 11. Summary damage detection and identification results.

Method	**Damage Detection**					
	False alarms	Missed damage cases				
		dam A	dam B	dam C	dam D	dam E
PSD	0/0/0	0/0/0	0/0/0	0/0/0	0/0/0	0/0/0
FRF	**1**/0/**2**	0/0/0	0/0/0	0/0/0	0/0/0	0/0/0
Mod. parameter†	0/0/0	0/0/0	0/0/0	0/0/0	0/0/0	0/0/0
Res. variance†	0/0/0	0/0/0	0/0/0	0/0/0	0/0/0	0/0/0
Res. likelihood†	0/0/0	0/0/0	0/0/0	0/0/0	0/0/0	0/0/0
Res. uncorrelatedness†	0/0/0	0/0/0	0/0/0	0/0/0	0/0/0	0/0/0
SPRT	0/0/0	0/0/0	0/0/0	0/0/0	0/0/0	0/0/0
Method	**Damage Identification**					
	Damage misclassification cases					
		dam A	dam B	dam C	dam D	dam E
PSD		0/0/0	0/0/0	0/0/0	0/0/0	0/0/0
FRF		**2**/1/**2**	0/0/0	0/0/0	0/0/0	0/0/0
Mod. parameter†		0/0/0	0/0/0	0/0/0	0/0/0	0/0/0
Res. variance†		0/0/0	0/0/0	0/0/0	0/0/0	0/0/0
Res. likelihood†		0/0/0	0/0/0	0/0/0	0/0/0	0/0/0
Res. uncorrelatedness†		0/0/0	0/0/0	0/0/0	0/0/0	0/0/0
SPRT		0/0/0	0/0/0	0/0/0	0/0/0	0/0/0

False alarms for responses Y1/Y2/Y3 out of 39 test cases each; †adjusted α.
Missed damages for responses Y1/Y2/Y3 out of 31 test cases each.
Damage misclassification for responses Y1/Y2/Y3 out of 31 test cases each.

tiple damages. In its more complete form in which damage may occur at an infinite number of locations on a continuum, the damage identification problem requires precise localization which – in the context of statistical time series methods – is possible only through the new Functional Model (FM) methods. These are more elaborate but also allow for damage magnitude estimation.

7 Concluding Remarks and Future Research

- Statistical time series SHM methods are capable of achieving damage detection, identification (including precise localization), and quantification (magnitude estimation) in both the *response-only* and *excitation-response* cases based on (i) random excitation and/or response signals, (ii) statistical model building, and (iii) statistical decision making under uncertainties.
- The methods may be classified as non-parametric or parametric. *Non-parametric* methods are generally simpler, while they mainly focus on the damage detection subproblem, although simple forms of the

damage identification subproblem may be also tackled. *Parametric* methods are more elaborate, as they necessitate the use of proper parameter estimation and model structure selection techniques. Yet, they offer potentially high performance along with more effective and precise damage identification (including localization) and quantification.

- The use of random excitation and/or vibration response signals is important and implies that signals obtained under *normal operating conditions* may be potentially employed, which is practically very important. This is further enhanced by the ability of the methods to work in the *lower frequency range*, as vibration signals obtained under normal operating conditions are often characterized by low frequency content.
- Two additional and practically important advantages of the methods is (i) the use of *simple and partial* (both space and bandwidth wise) dynamical models and (ii) a *limited number* of measured signals.
- The handling of uncertainties via proper statistical techniques is an additional asset.
- Sequential methods require, on average, a substantially smaller number of observations than their fixed sample size counterparts (Wald, 1947; Ghosh and Sen, 1991; Lehmann and Romano, 2008) and warrant further investigation. An added bonus is their direct suitability for on-line implementation, although other methods may be adapted as well.
- On the other hand, statistical time series SHM methods are limited to the identification of damage only to the extent allowed by the specific type of model employed, while they also require adequate user expertise. Another limitation relates to the requirement for vibration data records corresponding to the potential damage states of the structure in the baseline phase and in case that damage identification and estimation are sought. Such data may be difficult to obtain, but either laboratory scale models or analytical (like tuned finite element) models may be alternatively used.
- Further research is necessary for exploring the limits and applicability of the methods in tackling the less studied damage identification and estimation (quantification) subproblems, including the important multiple damage case. Effectively handling environmental effects, and distinguishing them from those of damage, is a critical issue warranting further investigation, as is the more effective handling of uncertainties. More automated methods and methods suitable for the multivariate (multi sensor) case (especially in conjunction with large

structures where dense sensor arrays may be used) need to be developed. Similarly, methods suitable for structures exhibiting nonlinear and/or time-varying (non-stationary) dynamics have received only limited attention and warrant further consideration.

Bibliography

D. E. Adams. *Health Monitoring of Structural Materials and Components.* John Wiley & Sons Inc., 2007.

D. E. Adams and C. R. Farrar. Classifying linear and nonlinear structural damage using frequency domain arx models. *Structural Health Monitoring*, 1(2):185–201, 2002.

D. Balageas, C. P. Fritzen, and A. Guemes, editors. *Structural Health Monitoring.* ISTE Ltd, 2006.

M. Basseville and I. V. Nikiforov. *Detection of Abrupt Changes.* PTR Prentice-Hall, 1993.

M. Basseville, M. Abdelghani, and M. Benveniste. Subspace-based faul detection algorithms for vibration monitoring. *Automatica*, 36(1):101–109, 2000.

M. Basseville, L. Mevel, and M. Goursat. Statistical model–based damage detection and localization: subspace–based residuals and damage-to-noise sensitivity ratios. *Journal of Sound and Vibration*, 275:769–794, 2004.

J. S. Bendat and A. G. Piersol. *Random Data: Analysis and Measurement Procedures.* Wiley–Interscience: New York, 3rd edition, 2000.

M. Benedetti, V. Fontanari, and D. Zonta. Structural health monitoring of wind towers: remote damage detection using strain sensors. *Smart Materials and Structures*, 20:13pp, 2011.

G. E. P. Box, G. M. Jenkins, and G. C. Reinsel. *Time Series Analysis: Forecasting & Control.* Prentice Hall: Englewood Cliffs, NJ, third edition, 1994.

E. P. Carden and J. M. Brownjohn. Arma modelled time–series classification for structural health monitoring of civil infrastructure. *Mechanical Systems and Signal Processing*, 22(2):295–314, 2008.

E. P. Carden and P. Fanning. Vibration-based condition monitoring: A review. *Structural Health Monitoring*, 3(4):355–377, 2004.

A. Deraemaeker, E. Reynders, G. De Roeck, and J. Kullaa. Vibration-based structural health monitoring using output-only measurements under changing environment. *Mechanical Systems and Signal Processing*, 22:34–56, 2008.

G. DeRoeck. The state-of-the-art of damage detection by vibration monitoring: the SIMCES experience. *Journal of Structural Control*, 10:127–134, 2003.

S. W. Doebling, C. R. Farrar, M. B. Prime, and D. W. Shevitz. Damage identification and health monitoring of structural and mechanical systems from changes in their vibration characteristics: A literature review. Technical Report LA-13070-MS, Los Alamos National Laboratory, 1996.

S. W. Doebling, C. R. Farrar, and M. B. Prime. A summary review of vibration–based damage identification methods. *Shock and Vibration Digest*, 30(2):91–105, 1998.

J. E. Doherty. Nondestructive evaluation. In A. S. Kobayashi, editor, *Handbook on Experimental Mechanics*, chapter 12. Society for Experimental Mechanics, 1987.

C. R. Farrar and S. W. Doebling. Using statistical analysis to enhance modal based damage identification. In J. M. Dulieu, W. J. Staszewski, and K. Worden, editors, *Structural Damage Assessment Using Advanced Signal Processing Procedures*, pages 199–211. Academic Press, Sheffield, 1997.

C. R. Farrar, S. W. Doebling, and D. A. Nix. Vibration–based structural damage identification. *The Royal Society – Philosophical Transactions: Mathematical, Physical and Engineering Sciences*, 359:131–149, 2001.

S. D. Fassois. Parametric identification of vibrating structures. In S.G. Braun, D.J. Ewins, and S.S. Rao, editors, *Encyclopedia of Vibration*, pages 673–685. Academic Press, 2001.

S. D. Fassois and J. S. Sakellariou. Time series methods for fault detection and identification in vibrating structures. *The Royal Society – Philosophical Transactions: Mathematical, Physical and Engineering Sciences*, 365:411–448, 2007.

S. D. Fassois and J. S. Sakellariou. Statistical time series methods for structural health monitoring. In C. Boller, F. K. Chang, and Y. Fujino, editors, *Encyclopedia of Structural Health Monitoring*, pages 443–472. John Wiley & Sons Ltd., 2009.

E. Figueiredo, G. Park, C .R. Farrar, K. Worden, and J. Figueiras. Machine learning algorithms for damage detection under operational and environmental variability. *Structural Health Monitoring*, 10(6):559–572, 2011.

C. P. Fritzen. Vibration-based techniques for structural health monitoring. In D. Balageas, C. P. Fritzen, and A. Guemes, editors, *Structural Health Monitoring*, pages 45–224. ISTE, 2006.

M. L. Fugate, H. Sohn, and C. R. Farrar. Vibration–based damage detection using statistical process control. *Mechanical Systems and Signal Processing*, 15(4):103–119, 2001.

F. Gao and Y. Lu. An acceleration residual generation approach for structural damage identification. *Journal of Sound and Vibration*, 319:163–181, 2009.

J. J. Gertler. *Fault Detection and Diagnosis in Engineering Systems.* Marcel Dekker, 1998.

B. K. Ghosh and P. K. Sen, editors. *Handbook of Sequential Analysis.* Marcel Dekker, Inc., New York, 1991.

A. Hera and Z. Hou. Application of wavelet approach for asce structural health monitoring benchmark studies. *Journal of Engineering Mechanics*, 130(1):96–104, 2004.

J. D. Hios and S. D. Fassois. Stochastic identification of temperature effects on the dynamics of a smart composite beam: assessment of multi–model and global model approaches. *Smart Materials and Structures*, 18(3): 035011 (15pp), 2009a.

J. D. Hios and S. D. Fassois. Statistical damage detection in a smart structure under different temperatures via vibration testing: a global model based approach. *Key Engineering Materials*, Vols. 413–414:261–268, 2009b.

J. D. Hios and S. D. Fassois. Stochastic identification under multiple operating conditions: Functionally pooled varma methods. In *Proceedings of the 15th Symposium on System Identification (SYSID)*, Saint-Malo, France, July 2009c.

Z. Hou, M. Noori, and R. St. Amand. Wavelet-based approach for structural damage detection. *Journal of Engineering Mechanics*, 126(7):677–683, 2000.

C. S. Huang, S. L. Hung, C. M. Wen, and T. T. Tu. A neural network approach for structural identification and diagnosis of a building from seismic response data. *Earthquake Engineering and Structural Dynamics*, 32:187–206, 2003.

H. Y. Hwang and C. Kim. Damage detection in structures using a few frequency response measurements. *Journal of Sound and Vibration*, 270: 1–14, 2004.

D. J. Inman, C. R. Farrar, V. Lopez Jr., and V. Steffen Jr., editors. *Damage Prognosis for Aerospace, Civil and Mechanical Systems.* John Wiley & Sons, 2005.

S. M. Kay. *Modern Spectral Estimation: Theory and Application.* Prentice Hall: New Jersey, 1988.

F. P. Kopsaftopoulos and S. D. Fassois. Identification of stochastic systems under multiple operating conditions: The vector dependent FP–ARX parametrization. In *Proceedings of 14th Mediterranean Conference on Control and Automation*, Ancona, Italy, 2006.

F. P. Kopsaftopoulos and S. D. Fassois. Vibration–based structural damage detection and precise assessment via stochastic functionally pooled models. *Key Engineering Materials*, 347:127–132, 2007.

F. P. Kopsaftopoulos and S. D. Fassois. Vibration based health monitoring for a lightweight truss structure: experimental assessment of several statistical time series methods. *Mechanical Systems and Signal Processing*, 24:1977–1997, 2010.

F. P. Kopsaftopoulos and S. D. Fassois. Scalar and vector time series methods for vibration based damage diagnosis in a scale aircraft skeleton structure. *Journal of Theoretical and Applied Mechanics*, 49(3):727–756, 2011.

F. P. Kopsaftopoulos and S. D. Fassois. A stochastic functional model based method for vibration based damage detection, precise localization, and magnitude estimation. *Mechanical Systems and Signal Processing, to appear*, 2012.

E. L. Lehmann and J. P. Romano. *Testing Statistical Hypotheses*. Springer, 3rd edition, 2008.

S. Liberatore and G. P. Carman. Power spectral density analysis for damage identification and location. *Journal of Sound and Vibration*, 274(3–5): 761–776, 2004.

L. Ljung. *System Identification: Theory for the User*. Prentice–Hall, 2nd edition, 1999.

Y. Lu and F. Gao. A novel time–domain auto–regressive model for structural damage diagnosis. *Journal of Sound and Vibration*, 283:1031–1049, 2005.

H. Lütkepohl. *New Introduction to Multiple Time Series Analysis*. Springer-Verlag Berlin, 2005.

G. Manson, K. Worden, and D. Allman. Experimental validation of a structural health monitoring methodology: part II, novelty detection on a gnat aircraft. *Journal of Sound and Vibration*, 259(2):345–363, 2003.

Z. Mao and M. Todd. A model for quantifying uncertainty in the estimation of noise-contaminated measurements of transmissibility. *Mechanical Systems and Signal Processing*, 2011. doi: doi:10.1016/j.ymssp.2011.10.002.

S. F. Masri, A. W. Smyth, A. G. Chassiakos, T. K. Caughey, and N. F. Hunter. Application of neural networks for detection of changes in nonlinear systems. *American Society of Civil Engineers (ASCE) Journal of Engineering Mechanics*, 126(7):666–676, 2000.

S. G. Mattson and S. M. Pandit. Statistical moments of autoregressive model residuals for damage localization. *Mechanical Systems and Signal Processing*, 20:627–645, 2006.

P. G. Michaelides and S. D. Fassois. Stochastic identification of structural dynamics from multiple experiments – epxerimental variability analysis. In *Proceedings of the ISMA Conference on Noise and Vibration Engineering*, Leuven, Belgium, September 2008.

D. Montalvão, N. M. M. Maia, and A. M. R. Ribeiro. A summary review of vibration–based damage identification methods. *Shock and Vibration Digest*, 38(4):295–324, 2006.

D. C. Montgomery. *Introduction to Statistical Quality Control*. John Wiley & Sons Inc., 2nd edition, 1991.

A.A. Mosavi, D. Dickey, R. Seracino, and S. Rizkalla. Identifying damage locations under ambient vibrations utilizing vector autoregressive models and mahalanobis distances. *Mechanical Systems and Signal Processing*, 26:254–267, 2012.

K. K. Nair and A. S. Kiremidjian. Time series based structural damage detection algorithm using gaussian mixtures modeling. *Journal of Dynamic Systems, Measurement, and Control*, 129:285–293, 2007.

K. K. Nair, A. S. Kiremidjian, and K. H. Law. Time series–based damage detection and localization algorithm with application to the asce benchmark structure. *Journal of Sound and Vibration*, 291:349–368, 2006.

H. G. Natke and C. Cempel. *Model-Aided Diagnosis of Mechanical Systems: Fundamentals, Detection, Localization, Assessment*. Springer-Verlag, 1997.

H. T. Nguyen and G. S. Rogers. *Fundamentals of Mathematical Statistics: Vols. I and II*. Springer–Verlag, New York, 1989.

C. K. Oh and H. Sohn. Damage diagnosis under environmental and operational variations using unsupervised support vector machine. *Journal of Sound and Vibration*, 328:224–239, 2009.

Z. K. Peng and F. L. Chu. Application of the wavelet transform in machine condition monitoring and fault diagnostics. *Mechanical Systems and Signal Processing*, 18:199–221, 2004.

A. G. Poulimenos and S. D. Fassois. Vibration-based on-line fault detection in non-stationary structural systems via a statistical model based method. In *Proceedings of the 2nd European Workshop on Structural Health Monitoring (EWSHM)*, pages 687–694, Munich, Germany, 2004.

P. S. Rao and C. Ratnam. Health monitoring of welded structures using statistical process control. *Mechanical Systems and Signal Processing*, 27:683–695, 2012.

D. D. Rizos, S. D. Fassois, Z. P. Marioli-Riga, and A. N. Karanika. Vibration–based skin damage statistical detection and restoration assessment in a stiffened aircraft panel. *Mechanical Systems and Signal Processing*, 22:315–337, 2008.

A. Rytter. *Vibration based inspection of civil engineering structures*. PhD thesis, Department of Building Technology and Structural Engineering, Aalborg University, Denmark, 1993.

J. S. Sakellariou and S. D. Fassois. Stochastic output error vibration–based damage detection and assessment in structures under earthquake excitation. *Journal of Sound and Vibration*, 297:1048–1067, 2006.

J. S. Sakellariou and S. D. Fassois. A functional pooling framework for the identification of systems under multiple operating conditions. In *Proceedings of 15th Mediterranean Conference on Control and Automation*, Athens, Greece, 2007.

J. S. Sakellariou and S. D. Fassois. Vibration based fault detection and identification in an aircraft skeleton structure via a stochastic functional model based method. *Mechanical Systems and Signal Processing*, 22: 557–573, 2008.

J. S. Sakellariou, K. A. Petsounis, and S. D. Fassois. Vibration analysis based on–board fault detection in railway vehicle suspensions: a feasibility study. In *Proceedings of First National Conference on Recent Advances in Mechanical Engineering*, Patras, Greece, 2001.

J. S. Sakellariou, K. A. Petsounis, and S. D. Fassois. On–board fault detection and identification in railway vehicle suspenions via a funcitonal model based method. In *Proceedings of the ISMA 2010 International Conference on Noise and Vibration Engineering*, Leuven, Belgium, 2002.

O. S. Salawu. Detection of structural damage through changes in frequency: a review. *Engineering Structures*, 19(9):718–72, 1997.

T. Söderström and P. Stoica. *System Identification.* Prentice–Hall, 1989.

H. Sohn. Effects of environmental and operational variability on structural health monitoring. *The Royal Society – Philosophical Transactions: Mathematical, Physical and Engineering Sciences*, 365:539–560, 2007.

H. Sohn and C. R. Farrar. Statistical process control and projection techniques for structural health monitoring. In *Proceedings of the European COST F3 Conference on System Identification and Structural Health Monitoring*, Madrid, Spain, 2000.

H. Sohn and C. R. Farrar. Damage diagnosis using time series analysis of vibration signals. *Smart Materials and Structures*, 10:446–451, 2001.

H. Sohn, C.R. Farrar, N.F. Hunter, and K. Worden. Structural health monitoring using statistical pattern recognition techniques. *Journal of Dynamic Systems, Measurement, and Control*, 123(4):706–711, 2001.

H. Sohn, D. W. Allen, K. Worden, and C. R. Farrar. Statistical damage classification using sequential probability ratio tests. *Structural Health Monitoring*, 2(1):57–74, 2003a.

H. Sohn, C. R. Farrar, F. M. Hemez, D. D. Shunk, D. W. Stinmates, and B. R. Nadler. A review of structural health monitoring literature: 1996–2001. Technical Report LA-13976-MS, Los Alamos National Laboratory, 2003b.

H. Sohn, D. W. Allen, K. Worden, and C. R. Farrar. Structural damage classification using extreme value statistics. *Journal of Dynamic Systems, Measurement, and Control*, 127:125–132, 2005.

M. D. Spiridonakos and S. D. Fassois. Vibration based fault detection in a time-varying link structure via non-stationary FS-VTAR models. In *Proceedings of the International Operational Modal Analysis Conference (IOMAC)*, Ancona, Italy, 2009.

W. J. Staszewski. Advanced data pre-processing for damage identification based on pattern recognition. *International Journal of Systems Science*, 31(11):1381–1396, 2000.

W. J. Staszewski. Structural and mechanical damage detection using wavelets. *Shock and Vibration Digest*, 30:457–472, 1998.

W. J. Staszewski and A. N. Robertson. Time-frequency and time-scale analyses for structural health monitoring. *The Royal Society – Philosophical Transactions: Mathematical, Physical and Engineering Sciences*, 365: 449–477, 2007.

W. J. Staszewski, C. Boller, and G. R. Tomlinson, editors. *Health Monitoring of Aerospace Structures: Smart Sensor Technologies and Signal Processing*. John Wiley & Sons, Chichester, U.K., 2004.

A. Stuart and J. K. Ord. *Kendalls Advanced Theory of Statistics: Vol 1. Distribution Theory*. Oxford University Press, New York, 5th edition, 1987.

T. Uhl and K. Mendrok. Overview of modal model based damage detection methods. In *Proceedings of the ISMA 2004 International Conference on Noise and Vibration Engineering*, Leuven, Belgium, 2004.

A. Wald. *Sequential Analysis*. Wiley, New York, 1947.

Z. Wei, L. H. Yam, and L. Cheng. NARMAX model representation and its application to damage detection for multi-layer composites. *Composite Structures*, 68:109–117, 2005.

K. Worden. Structural fault detection using a novelty measure. *Journal of Sound and Vibration*, 201(1):85–101, 1997.

K. Worden and G. Manson. Experimental validation of a structural health monitoring methodology: part I. novelty detection on a laboratory structure. *Journal of Sound and Vibration*, 259(2):323–343, 2003.

K. Worden, G. Manson, and N. R. J. Fieller. Damage detection using outlier analysis. *Journal of Sound and Vibration*, 229(3):647–667, 2000.

A.M. Yan, P. de Boe, and J. C. Golinval. Structural damage diagnosis by kalman model based on stochastic subspace identification. *Structural Health Monitoring*, 3(2):103–119, 2004.

Q. W. Zhang. Statistical damage identification for bridges using ambient vibration data. *Computers and Structures*, 85:476–485, 2007.

H. Zheng and A. Mita. Two–stage damage diagnosis based on the distance between arma models and pre–whitening filters. *Smart Materials and Structures*, 16:1829–1836, 2007.

Y. Zou, L. Tong, and G. P. Steven. Vibration-based model-dependent damage (delamination) identification and health monitoring for composite structures. *Journal of Sound and Vibration*, 230:357–378, 2000.

A Appendix: Central limit theorem and statistical distributions associated with the normal

A.1 The Central Limit Theorem (CLT)

Theorem A.1 (The Central Limit Theorem (Stuart and Ord, 1987; Nguyen and Rogers, 1989; Montgomery, 1991)). *Let $Z_1, Z_2, \dots Z_n$ designate mutually independent random variables each with mean μ_k and (finite) variance σ_k^2. Then, for $n \longrightarrow \infty$ the distribution of the random variable $X = \sum_{k=1}^{n} Z_k$ approaches the Gaussian distribution with mean $E\{X\} = \sum_{k=1}^{n} \mu_k$ and variance $var[X] = \sum_{k=1}^{n} \sigma_k^2$.* □

A.2 The χ^2 distribution

Let $Z_1, Z_2, \dots Z_n$ designate mutually independent, normally distributed, random variables, each with mean μ_k and standard deviation σ_k. Then the sum:

$$X = \sum_{k=1}^{n} \left(\frac{Z_k - \mu_k}{\sigma_k} \right)^2 \tag{A.1}$$

is said to follow a (central) chi-square distribution with n degrees of freedom ($X \sim \chi^2(n)$). Its mean and variance are $E\{X\} = n$ and $\text{var}[X] = 2n$, respectively. Notice that imposing p equality constraints among the random variables $Z_1, Z_2, \dots Z_n$ reduces the set's effective dimensionality, and thus the number of degrees of freedom, by p (Stuart and Ord, 1987, pp. 506–507).

For $n \longrightarrow \infty$ the $\chi^2(n)$ distribution tends to normality (Stuart and Ord, 1987, p. 523).

The sum $X = \sum_{k=1}^{n} Z_k^2/\sigma_k^2$ is said to follow non-central chi-square distribution with n degrees of freedom and non-centrality parameter $\lambda = \mu_k^2/\sigma_k^2$. This distribution is designated as $\chi^2(n; \lambda)$ (Nguyen and Rogers, 1989, Vol. II p. 33).

Let $\boldsymbol{x} \in \mathbb{R}^n$ follow n-variate normal distribution with zero mean and covariance $\boldsymbol{\Sigma}$ ($\boldsymbol{x} \sim \mathcal{N}(\mathbf{0}, \boldsymbol{\Sigma})$). Then the quantity $\boldsymbol{x}^T \boldsymbol{\Sigma}^{-1} \boldsymbol{x}$ follows (central) chi-square distribution with n degrees of freedom (Söderström and Stoica 1989, p. 557, Stuart and Ord 1987, pp. 486–487, Gertler 1998, p. 120).

A.3 The Student's t distribution

Let Z be the standard (zero mean and unit variance) normal variable. Let X follow a (central) chi-square distribution with n degrees of freedom and be independent of Z. Then the ratio:

$$T = \frac{Z}{\sqrt{X/n}} \tag{A.2}$$

is said to follow a Student or t (central) distribution with n degrees of freedom (central because it is based on a central chi-square distribution; Nguyen and Rogers 1989, Vol. II p. 34). Its mean and variance are $E\{T\} = 0$ $(n > 1)$ and $\text{var}[T] = \frac{n}{n-2}$ $(n > 2)$, respectively (Stuart and Ord, 1987, p. 513).

The (central) t distribution approaches the standard normal distribution $\mathcal{N}(0,1)$ as $n \longrightarrow \infty$ (Stuart and Ord, 1987, p.523).

A.4 The Fisher's F distribution

Let X_1,X_2 be mutually independent random variables following (central) chi-square distributions with n_1, n_2 degrees of freedom, respectively. Then the ratio:

$$F = \frac{X_1/n_1}{X_2/n_2} \tag{A.3}$$

is said to follow a (central) F distribution with n_1, n_2 degrees of freedom ($F \sim \mathcal{F}(n_1, n_2)$; central because it is based on central chi-square distributions; Nguyen and Rogers 1989, Vol. II p. 34). Its mean and variance are $E\{F\} = \frac{n_2}{n_2-2}$ $(n_2 > 2)$ and $\text{var}[F] = \frac{2n_2^2(n_1+n_2-2)}{n_1(n_2-2)^2(n_2-4)}$ $(n_2 > 4)$, respectively (Stuart and Ord, 1987, p. 518).

Note that for the distribution's $1-\alpha$ critical point $f_{1-\alpha}(n_1, n_2) = 1/f_\alpha(n_2, n_1)$.

The (central) F distribution approaches normality as $n_1, n_2 \longrightarrow \infty$. For $n_2 \longrightarrow \infty$ $n_1 F$ approaches a (central) chi-square distribution with n_1 degrees of freedom (Stuart and Ord, 1987, p. 523).